Quaternary Science Reviews 285 (2022) 107509

Contents lists available at ScienceDirect

Quaternary Science Reviews

journal homepage: www.elsevier.com/locate/quascirev

Insights into changing coastlines, environments and marine hunter-gatherer lifestyles on the Pacific coast of South America from the La Yerba II shell midden, Río Ica estuary, Peru

David G. Beresford-Jones [a, b, *], David E. Friesem [c, d, e], Fraser Sturt [f], Alexander Pullen [g], George Chauca [h], Justin Moat [i], Manuel Gorriti [j], Patricia K. Maita [k], Delphine Joly [l], Oliver Huaman [h], Kevin J. Lane [m], Charles French [b]

[a] Heinz Heinen Centre for Advanced Study, University of Bonn, Heussallee 18–24, 53113, Bonn, Germany
[b] McDonald Institute for Archaeological Research, University of Cambridge, Downing Street, CB2 3ER, Cambridge, UK
[c] Department of Maritime Civilizations, School of Marine Sciences, University of Haifa, Haifa, 3498838, Israel
[d] Recanati, Institute for Maritime Studies, University of Haifa, Haifa, 3498838, Israel
[e] Haifa Center for Mediterranean History, University of Haifa, Haifa, 3498838, Israel
[f] University of Southampton, Department of Archaeology, Avenue Campus, Highfield, Southampton, SO17 1BF, UK
[g] Pre-Construct Archaeology, The Granary, Rectory Farm, Pampisford, Cambridgeshire, CB22 3EN, UK
[h] Universidad Nacional Mayor de San Marcos, Escuela Profesional de Arqueología, Av. Universitaria s/n., Lima, Peru
[i] Royal Botanic Gardens, Kew, Richmond, Surrey, TW9 3AE, UK
[j] Proyecto Especial Arqueológico Caral-Supe, Las Lomas de la Molina 327, urb. Las Lomas de la Molina Vieja, Lima, 12, Peru
[k] Colección de Antropología Física, Museo Nacional de Arqueología, Antropología e Historia del Perú, Plaza Bolívar s/n, Pueblo Libre, Lima, Peru
[l] Department of Environment and Geography, Environment Building, University of York, Wentworth Way, Heslington, York, UK
[m] Consejo Nacional de Investigación de Ciencia y Tecnología (CONICET), Instituto de las Culturas (IDECU), Universidad de Buenos Aires, Moreno 350, Cuidad de Buenos Aires, Argentina

ARTICLE INFO

Article history:
Received 20 December 2021
Received in revised form
16 March 2022
Accepted 4 April 2022
Available online 27 April 2022

Handling editor: Mira Matthews

Keywords:
Middle Preceramic
Holocene
Pacific coast South America
Shell midden archaeology
Marine hunter-gatherers
Geoarchaeology
Floor surfaces
Relative sea level

ABSTRACT

Shell middens are conspicuous manifestations of the exploitation of rich, sustainable, easily seen and harvested marine resources that, worldwide, enabled hunter-gatherers to reduce mobility and increase population and social complexity. Globally, known sites tend to cluster chronologically around 6 k BP, after slowing eustatic sea-level rise, although the Pacific coast of South America offers some rare earlier exceptions.

We report investigations of La Yerba II, a Middle Preceramic shell matrix site on the Río Ica estuary, south coast Peru. These show how, beginning around 7000 Cal BP, over 4.5 m of stratigraphy accumulated in less than 500 years. Consisting of prepared surfaces, indurated floors and the ashy interiors of wind shelters and their associated midden deposits, alternating with phases of abandonment, this was the outcome of an intense rhythm of repeated occupations by logistically mobile marine hunter-gatherers. Final phases, dominated by *Mesodesma* surf clams, mark change towards more task-specific activities.

La Yerba II's topographic position and well-preserved cultural and environmental markers provide insight into the local history of relative sea level change and changing marine hunter-gatherer lifestyles during a period critical to the transition to sedentism and the formation of new estuarine and beach habitats following the stabilisation of eustatic sea-levels.

* Corresponding author. Heinz Heinen Centre for Advanced Study, University of Bonn, Heussallee 18–24, 53113 Bonn, Germany.
E-mail address: david.beresfordjones@gmail.com (D.G. Beresford-Jones).

https://doi.org/10.1016/j.quascirev.2022.107509

1. Introduction

The long prelude to the emergence of agriculture was characterised worldwide by a widening use of resources by hunter-gatherers: a so-called Broad Spectrum Revolution that came hand in hand with increasing sedentism, population density, technological innovation and social complexity (e.g. Flannery, 1969; Zeder, 2012). Typically these seem to have unfolded in 'ecotonally-diverse' settings — places where different ecosystems conjoined — where people could reduce mobility by exploiting diverse and seasonally abundant resources according to rounds of logistical, rather than residential, mobility (*sensu* Binford, 1980).

Coasts are quintessential such environments: the intersection of very different, often highly productive, habitats. Estuaries, as the nexus of marine and freshwater ecosystems, enjoy high levels of nutrient influx from each (Day et al., 2012). Coastal productivity can be among the highest in the world, equivalent to those of tropical rainforests (McLusky and Elliott, 2004), providing sustainable, easily seen resources, many of which can be harvested without particular skills by all segments of a population (De Vynck et al., 2016). Indeed, across the globe broad spectrum Mesolithic economies relied on the systematic exploitation of aquatic and marine resources (e.g. Binford, 1968; Stiner, 2001; Bar-Yosef Mayer and Zohar, 2010; Bicho et al., 2011; Jerardino, 2010; Lewis et al., 2020). The archaeological footprint of this activity, however, is much distorted by the impacts of sea-level change (Bailey and Hardy, 2021).

As temperatures warmed into the Holocene, sea levels rose by up to 120m, inundating coastal landscapes and altering their geography, sometimes dramatically, according to local bathymetry, isostatic and tectonic factors (Harff et al., 2016). It is no surprise then that, worldwide, the earliest shoreline archaeological sites tend to cluster around 5800 BP: the date by which eustatic seas levels began to stabilize. Important exceptions (e.g. Sandweiss et al., 1998; Fisher et al., 2020) serve to prove the rule that, along the world's coastlines, the exposed Holocene archaeological record is an artefact of a point in time, or as Bradley, (1984, 5) puts it for Britain, where almost 40% of Mesolithic landscapes are today submerged, a 'picture dominated by its frame'.

Along many of the world's coasts that picture is most conspicuously manifest in ancient and sometimes massive, anthropogenic accumulations of shells. Originally conceived of as merely homogeneous dumps of food waste, many of these *kjokkenmoeddinger* shell midden, or more generally 'shell-matrix' sites (see definitions in Villagran, 2019: 345), are now understood to be the outcome of successive episodes of activity offering deep-time archives of prehistoric coastal hunter-gatherer ecology and economy. Beyond quotidian subsistence, however, they are increasingly also interpreted as offering insights into ancient ritual behaviour, social dynamics and even early monumentality (e.g. Gaspar et al., 2008; Dillehay et al., 2012; Klokler, 2014; Marean, 2014; Jerardino and Navarro, 2018).

One such location is the Pacific coast of South America where a long Mesolithic-like Middle Preceramic (or 'Middle Archaic') Period culminated in the fluorescence of one of humanity's rare hearths of agriculture and pristine civilisation. The littoral itself here is one the world's driest deserts but is traversed by lush riverine oases along watercourses that rise along the western flanks of the Andes, while offshore cold upwellings driven by the Humboldt Current support a prodigious marine food chain and the world's richest fishery (FAO, 2014). Exploitation of these marine resources is documented by some of the earliest, best-preserved shell-matrix sites in the Americas. Here site preservation is enhanced by the region's hyperarid climate but also because a narrow, steep continental shelf, particularly north of 5°S and south of 14°S, has meant relatively little horizontal shoreline displacement following eustatic sea-level change through the Holocene (Sandweiss, 2009). As in other places with similar morphology, such as parts of the coast of South Africa (e.g. Cawthra et al., 2018; Fisher et al., 2020; Esteban et al., 2020), this has resulted in episodic preservation of sites along this Pacific littoral dating back to the Terminal Pleistocene (Engel, 1981, 1991; Sandweiss et al., 1998; Sandweiss, 2003; Lavallée and Julien, 2012; Beresford-Jones et al., 2015; Salazar et al., 2015; Dillehay, 2017; Power et al., 2021).

Changes in relative sea-level (RSL) are driven by eustatic, isostatic, tectonic and more local factors such as sedimentary regimes. The variable geology, geomorphology and complex tectonic history of the Pacific coast of Peru make it difficult to apply a generalised sea-level curve to the region. Moreover, as Borreggine et al. (2022) note, simplistic 'bath tub' modelling of sea-level change that give no consideration to critical local factors can hinder rather than illuminate interpretations of coastline archaeological potential. Thus, while the submerged continental shelf here is comparatively narrow, past coastal configuration and how it relates to specific archaeological sites remains less clear.

The region spans the convergence between the Nazca and South American Plates, driving significant tectonic activity (Hsu, 1992; Saillard et al., 2011; Garrett et al., 2020), and with it land-surface deformation and associated RSL change. A history of this activity is captured within the geological record at the local to regional level, with significant uplift recorded along and around the Nazca Ridge (Hsu, 1992; Saillard et al., 2011), and frequent megathrust earthquakes impacting the wider region. Further south in Chile there is increasing isostatic impact on RSL change due to the melt and retreat of the Patagonian Ice sheet, leading to regional uplift since the last glacial maximum. These factors, as Bailey and Flemming, (2008, 2158) note, call for more local-level investigations.

Part of the challenge of working in this area, however, is the comparative scarcity of RSL data (Blanco-Chao et al., 2014, 161) from which to resolve regional sea-level histories. For the Pleistocene work has been done on dating exposed marine terraces and strandlines (Goy et al., 1992; Hsu, 1992; Saillard et al., 2011; Regard et al., 2021), with the staircase sequence of marine terraces at Chala Bay dating back to Marine Isotope Stage (MiS) 19 providing a key sequence for regional comparisons. Recently Freisleben et al. (2021) have used this to map the extent of highstand terraces along the Pacific coast of South America from 1° N to 40° S, using published dates to constrain terrace-age estimates and providing insight into variable uplift rates along this coast over the last 125 kyr (Fig. 1).

For the Holocene, however — the time of principle archaeological interest in the Americas — data for RSL change along the Peruvian and Chilean coasts is very limited. There has, as Garrett et al. (2020, 1) note, been no 'systematic attention' to the RSL history of Chile aside from broad data compilations (Isla et al., 2012), a lacuna they begin to address with their sea-level database for the coast of Chile using an internationally comparable approach. This database, complied *inter alia* from critical review of key archaeological sites and their relationship to past sea-levels, gives 79 sea-level index points and 87 limiting points spanning the period 11,000 years ago to present day, but accepts only a single marine limiting point for all northern Chile at Caleta Michilla (22° 43′ S, Fig. 1). No such resource yet exists for the coast of Peru. Garrett et al.'s work highlights the need for more detailed understanding of Holocene sea level change along this littoral, not least because of the many important coastal archaeological sites it would help to contextualise. For instance, while most radiocarbon dates for Middle Archaic shell matrix sites on the north coast of Chile cluster after 6000 cal BP (Salazar et al., 2015: Table 1; Castro et al., 2016: Table 1, Santoro et al., 2017: Table 2), two sites — Zapatero and

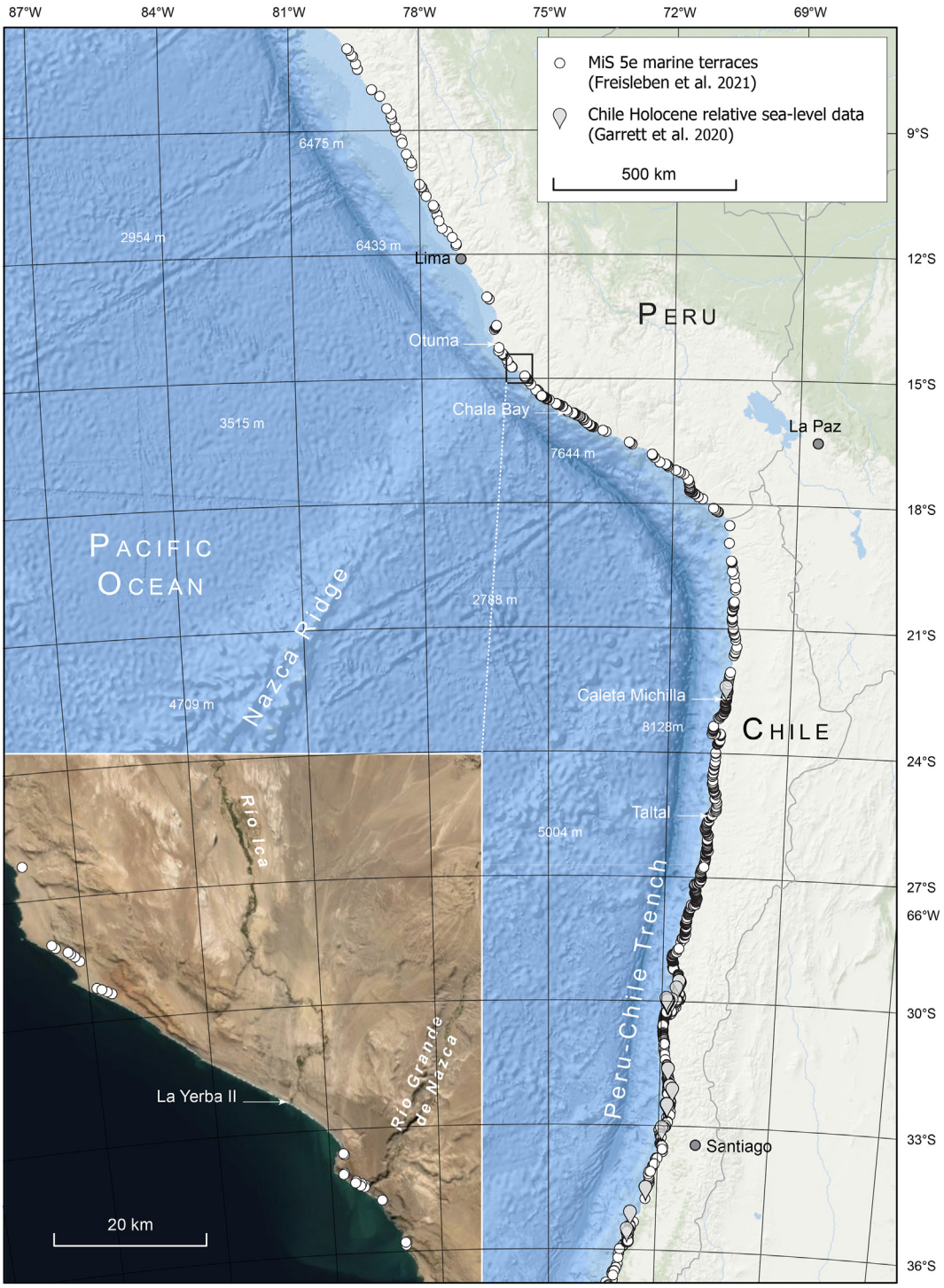

Fig. 1. Map of Pacific coast of Chile and Peru showing study area (inset) and locations mentioned in text in relation to known exposures of MiS 5e terraces (from Freisleben et al., 2021) and Chilean Holocene sea-level index points (from Garrett et al., 2020). Data sources: ESRI, GEBCO, DeLorme, NatreVue, EarthStar Geographics.

Morro Colorado — have reliably dated contexts of between 7500 and 7000 cal BP (Power et al., 2021; Salazar et al., 2015), both near Taltal, some 300 km south of Caleta Michilla's uplifted marine terrace 5.5 m above mean sea level and dated to 7200 BP (Garrett et al., 2020: 8). Few of the shell-midden sites along this Pacific littoral have, however, been investigated with the chronostratigraphic and geoarchaeological detail necessary to understand what their situations may imply about local sea level changes or their often complex formation processes (e.g. Waselkov, 1987; Stein, 1992; Jerardino, 2010).

Elsewhere in South America, two other, contrasting contexts exemplify the poles of a continuum of interpretation for how shell middens can form: the often monumental *sambaquis* shell mounds on the Atlantic seaboard of Brazil, Santa Catarina, some up to 50 m high and among the largest anywhere; and the far smaller, yet stratigraphically complex shell-middens along the shores of Tierra

Table 1
Field descriptions of La Yerba II contexts selected for geoarchaeological analyses.

Context	Depth (m top of unit from surface/m asl)	Description	Field Characterisation	Equivalent Contexts		
				Trench 1	Trench 3	Trench 4
TRENCH 3						
SU 1053	0.20/20.12	0.30 m thick layer of sandy-shell, > 80% *Mesodesma donacium* shells, other marine shell, fish bones, frequent small fragments of crustacean and few fragments of marine mammal bone and carbonised plants remains.	Type V	SU 1001 SU 1002	SU 1054	
SU 1050	0.50/19.82	0.13m thick lens of dark grey, indurated charcoal rich sand. Frequent mollusc shell, crustacean and plant fibres.	Type III	SU 1015 SU 1008	SU 1057 SU 1073 SU 1079 SU 1081	SU 1064 SU 1070
SU 1060	0.44/19.88	0.52 m thick layer of laminated, unconsolidated greyish-yellow sands with frequent mollusc shell, crustacean and plant fibres.	Type II	SU 1004 SU 1005 SU 1007 SU 1010 SU 1016 SU 1017 SU 1018	SU 1072 SU 1075 SU 1052	SU 1063 SU 1069
SU 1073	1.02/19.30	0.10 m thick layer of dark-grey to black consolidated sandy-ash with frequent micro charcoals and fragmented charred plant remains and few fragmented clam shells and crustaceans.	Type III	See SU 1050 above		
SU 1078	1.23/19.09	0.10m thick layer (0.40 × 0.20 m) of brown indurated (organic?) silt	Type IV	SU 1014	SU 1054 SU 1071	
SU 1079	1.20/19.12	0.20m thick layer poorly consolidated mid grey ashy-sand with frequent inclusions of fragmentary plant remains and small fragments of crustacea. Stratigraphically equivalent to SU 1052.	Type III	See SU 1050 above		
SU 1081	2.16/18.16	0.04 m thick layer of consolidated dark grey ashy and charcoal rich sand. Few plant remains and small fragments of crustaceans.	Type III	See SU 1050 above		
SU 1083	2.36/17.96	0.06 m thick layer of consolidated mid brownish-yellow sand.	Type IV	See SU 1078 above		
TRENCH 4 ('Carré Trench')						
SU 1062	0.01/20.82	0.25 m thick moderately poorly consolidated, mid brown silty sand with few marine shells, desiccated reed stem fragments, crustacean fragments and feathers.	Type II	See SU 1060 above		
SU 1063	0.29/20.54	0.15 m thick poorly consolidated, mid-grey ashy sand with frequent crustacean fragments, very few marine and terrestrial shell fragments.	Type II	See SU 1060 above		
SU 1064	0.41/20.42	0.08 m thick poorly consolidated dark grey ashy sand with frequent crustacean fragments and very few large charcoals.	Type III	See SU 1050 above		
SU 1068	0.88/19.95	0.15m thick layer of sand and *in situ* reed matting with occasional sub-angular cobbles.	Collapsed areesh wind shelter			
SU 1070	0.36/20.47	0.25 m thick layer of poorly consolidated greyish sand with c. 0.05 m thick weakly distinct ash stained lenses. Very few marine mammal bone, few mollusc shell, fragmentary crustacean shell and desiccated plant remains.	Type III	SU 1006 SU1009 SU 1011 SU1012 SU 1019	SU 1055 SU 1056 SU1058 SU 1059 SU 1076 SU 1077 SU 1082	SU 1061 SU1062 SU 1066 SU 1067

de Fuego far to the south. For whereas the latter are understood in the light of Yamana (or Yaghan) ethnography (e.g. Lothrop, 1928) as the outcome of unintentional, gradual accumulation of food waste arising through successions of short-lived, repeated occupations over great time depth by relatively small-scale, mobile marine forager society(ies) (Balbo et al., 2010; Villagran et al., 2011; Ozán et al., 2015; Zangrando et al., 2021), the Santa Catarina *sambaquis* are interpreted to be the outcome of much faster, intentional heaping up and reworking of shells to construct monumental platforms, typically taken to connote larger, more sedentary and socially complex populations (e.g. Fish et al., 2000; Neves and Wesolowski, 2002; Gaspar et al., 2008; Klokler, 2014; Villagran, 2014, 2019). Such dichotomies can apply to interpretations of the same site. Large 'megamiddens' on the west coast of South Africa were originally explained using Kalahari San ethnography as the vestiges of unchanging patterns of brief seasonal mollusc gathering visitations by small populations ordinarily resident inland (e.g. Parkington et al., 2009). Diverse lines of new evidence, however, now suggest them to be the more complex outcome of increasing population density and more permanent residence after around 3000 BP (Jerardino, 2010, 2012). These cases illustrate how, since shell-middens are the outcome of intensity, rhythm *and* time-depth of human activity in combination with natural processes, their size and form *per se* are only crude criteria by which to understand their formation (Marquardt, 2010; Karkanas et al., 2015). Indeed, reconstructing the processes and rate of shell-midden accumulation, and thereby the scale and nature of the social processes that underlie their formation, present problems that are far from trivial, requiring a detailed understanding of their stratigraphy (cf. Voorhies, 2015: 201), within a well-resolved chronological framework (cf. Kennett and Culleton, 2012): each all too often lacking in interpretations.

Geoarchaeological analyses have proven critical to interpreting complex shell-midden stratigraphies in Morocco (Linstädter and Kehl, 2012), Portugal (Stiner et al., 2003; Aldeias and Bicho, 2016; Duarte et al., 2019), Mexico (Voorhies, 2015), South Africa (Karkanas et al., 2015) and the USA (Stein et al., 2011; Thompson et al., 2016). In particular, micromorphology offers a high-resolution window into archaeological and natural sediments to reveal the sequences of human activities and natural processes behind shell midden formation and the post-depositional processes since (Karkanas and Goldberg, 2018). Villagran (2019) offers a recent, comprehensive review of the different micromorphological micro-facies associated with particular episodes of deposition and post-depositional alterations in Fuegian and Brazilian shell middens.

Table 2
La Yerba II radiocarbon dates modelled as phases in sequence.

OxCal v4.4.4 Bronk Ramsey (2021); r:5 ShCal20 atmospheric curve (Hogg et al., 2020)														
Lab. Ref	Context	Dated Material	Radiocarbon Date		Calibrated Unmodelled				Calibrated Modelled				Indices	
			$\delta^{13}C$	C^{14} Age	(yrs BP ±1σ)				(yrs BP ±1σ)				A	C
				(yrs)	From	To	%	median	From	To	%	median		
TRENCH 1														
Sequence														
Boundary Start Trench 1									**6740**	**6585**	**95.4**	**6672**		**97.6**
OxA-29965	SU 1002	Desiccated plant fibre cord	−24.7	5937 ± 31	6842	6638	95.4	6719	6743	6645	95.4	6692	113.8	99.2
OxA-29966	SU 1004	Desiccated plied plant fibre cord	−20.9	5914 ± 32	6793	6564	95.4	6701	6752	6661	95.4	6709	125.1	99.4
OxA-29967	SU 1005	Wood charcoal fragment	−27.4	5943 ± 33	6847	6640	95.4	6726	6771	6679	95.4	6726	118.6	99.7
Phase SU 1007														
OxA-29968	SU 1007a	Desiccated reed stem (*Phragmitis* sp.)	−23.3	6039 ± 32	6844	6573	95.4	6713	6797	6699	95.4	6754	90	99.8
OxA-29969	SU 1007b	Desiccated reed stem (*Phragmitis* sp.)	−23.3	5930 ± 33	6948	6740	95.4	6842	6829	6732	95.4	6774	77.8	99.9
OxA-29970	SU 1008	Desiccated plied plant fibre cord	−22.8	5934 ± 31	6841	6636	95.4	6717	6797	6700	95.4	6755	91.5	99.7
OxA-29971	SU 1009	Wood charcoal fragment	−28.0	6033 ± 32	6947	6737	95.4	6835	6848	6755	95.4	6800	113.6	99.9
OxA-29972	SU 1010	Charred *Scirpus* sp. rhizome	−25.3	6039 ± 31	6946	6742	95.4	6841	6868	6780	95.4	6816	122.7	99.8
OxA-29973	SU 1013	Charred *Scirpus* sp. rhizome	−26.4	6069 ± 32	6987	6749	95.4	6876	6879	6794	95.4	6832	104	99.9
Phase SU 1015														
OxA-29974	SU 1014	Charred *Scirpus* sp. rhizome	−25.9	6022 ± 31	6943	6685	95.4	6824	6914	6807	95.4	6859	107.9	99.9
OxA-29975	SU 1015	Charred *Scirpus* sp. rhizome	−25.9	5988 ± 33	6887	6672	95.4	6779	6907	6807	95.4	6855	68.5	99.9
OxA-29976	SU 1016	Charred *Scirpus* sp. rhizome	−26.3	6013 ± 32	6937	6679	95.4	6814	6947	6838	95.4	6888	60.5	99.8
Phase SU 1017														
OxA-29977	SU 1017	Desiccated reed stem (*Phragmitis* sp.)	−24.9	6218 ± 31	7235	6955	95.4	7074	7074	6891	95.4	6982	58.2[a]	99.4
OxA-29978	SU 1018	Desiccated plied plant fibre cord	−22.5	6165 ± 30	7159	6901	95.4	7014	7056	6886	95.4	6964	99.2	99.7
Boundary End Trench 1									**7130**	**6903**	**95.4**	**7011**		**95.9**
Maximum Time Span (yrs)						**671**		**373**		**545**		**339**		
													A model	80.8
													A overall	78.5
TRENCH 3														
Sequence														
Boundary Start Trench 3									**6775**	**6530**	**95.4**	**6670**		**97.9**
OxA-29942	SU 1053	Wood charcoal (cf. *Prosopis* sp.)	−27.7	5872 ± 30	6743	6503	95.4	6649	6776	6607	95.4	6696	99.9	99.6
OxA-29940	SU 1050	Desiccated *Scirpus* sp. rhizome	−26.6	5964 ± 31	6879	6662	95.4	6751	6774	6666	95.4	6722	106.2	99.8
OxA-29941	SU 1072	Desiccated vegetable fibre cord	−26.9	5944 ± 31	6847	6643	95.4	6727	6785	6685	95.4	6740	111.7	99.9
OxA-29943	SU 1073	Desiccated *Scirpus* sp. rhizome	−26.2	5993 ± 31	6888	6674	95.4	6785	6823	6706	95.4	6759	123.6	99.9
OxA-29979	SU 1076	Desiccated flower head *Scirpus* sp.	−25.9	5972 ± 31	6882	6666	95.4	6761	6841	6735	95.4	6778	121.1	99.9
Phase SU 1079														
OxA-29980	SU 1079	Desiccated gourd fragment	−25.1	6029 ± 32	6946	6736	95.4	6831	6888	6745	95.4	6809	111.8	99.7
OxA-29944	SU 1079	Desiccated gourd fragment	−24.2	6029 ± 31	6947	6735	95.4	6831	6888	6745	95.4	6809	112.3	99.7
Boundary End Trench 3									**6975**	**6747**	**95.4**	**6845**		**97.8**
Maximum Time Span (yrs)						**444**		**183**		**445**		**175**		
													A model	135.1
													A overall	135.3
TRENCH 4 – Carré Trench[b]														
Sequence														
Boundary Start Trench 4									**6737**	**6142**	**95.4**	**6561**		**95.2**
OS-60543	SU 1062	Charcoal	−29.7	5840 ± 35	6732	6492	95.4	6604	6733	6505	95.4	6632	102.9	99.5
OS-60556	SU 1063	Charcoal	−28.3	5940 ± 45	6884	6567	95.4	6726	6778	6627	95.4	6692	113.2	99.7
Phase Trench Bottom														
OS-60544	SU 1068	Charcoal	−27.1	6070 ± 30	6986	6751	95.4	6877	6948	6738	95.4	6829	88.7	99.1
OS-60564	SU 1069	Charcoal	−27.6	5900 ± 40	6794	6505	95.4	6685	6834	6659	95.4	6731	96.6	99.6
Boundary End Trench 4									**7357**	**6690**	**95.4**	**6903**		**95.9**
Maximum Time Span (yrs)						**494**		**273**		**1215**		**342**		
													A model	99.9
													A overall	99.9

Notes.
[a] Agreement index <60%.
[b] Source for uncalibrated radiocarbon data: Carré et al., *Science* 345, 1045–1048 (2014).

Meanwhile, Bayesian statistical analysis of radiocarbon dates using the OxCal program (Bronk Ramsey, 2009) enables coherent chronologies to be resolved for complex shell-midden stratigraphies by using radiocarbon dates from culturally significant archaeological contexts in presumed contextual associations to model and test the coherence of those *a priori* stratigraphies through agreement indices (e.g. Kennett and Culleton, 2012). Once such modelling justifies a statistically coherent *a posteriori*

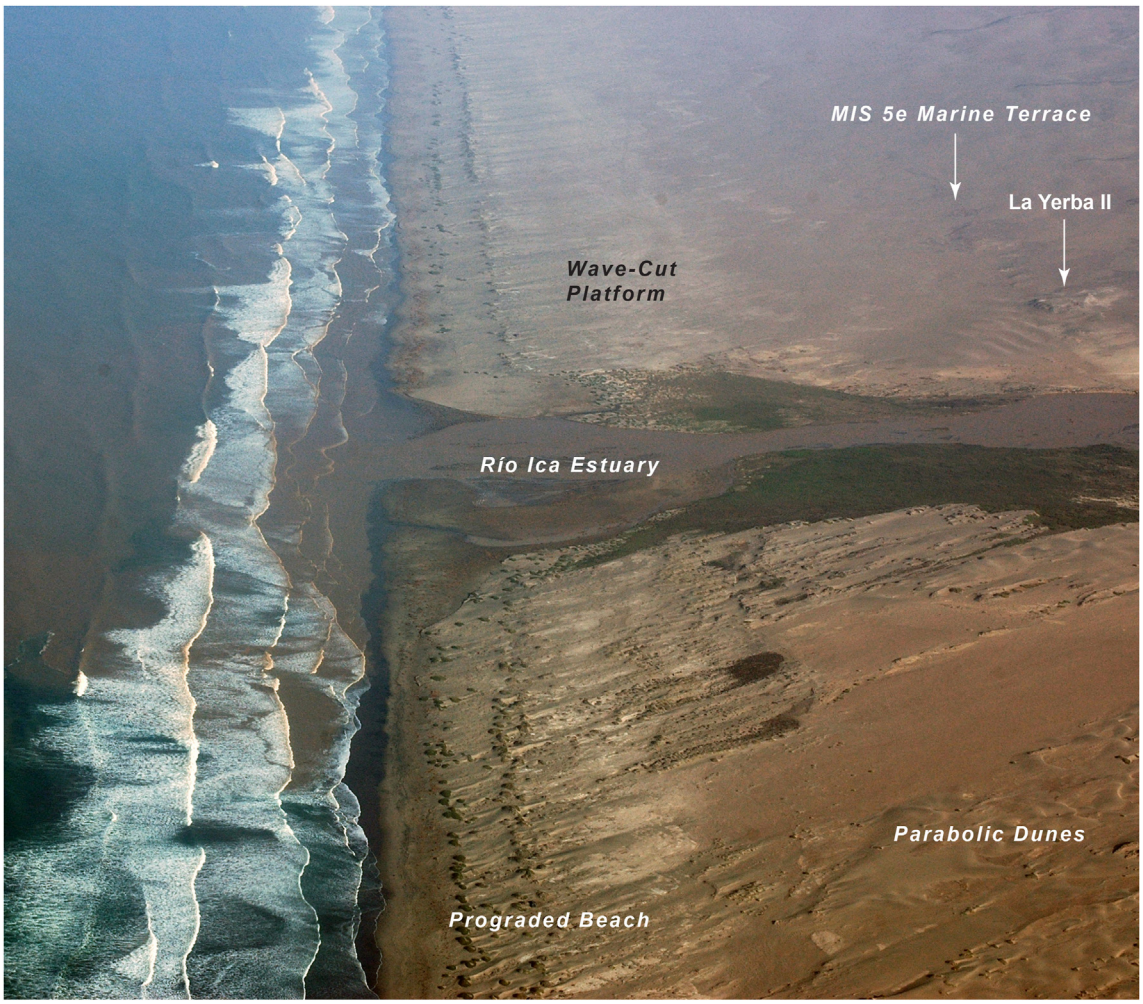

Fig. 2. View north of the context of the La Yerba II shell midden, Río Ica estuary, south coast Peru.

stratigraphic relationship between radiocarbon dates, this can be used to constrain the probability distributions of their calibrated ranges, typically resulting in tighter age estimates. Such detailed chronostratigraphic analyses have proven critical to understanding the formation processes in complex shell midden sites in the US (Kennett and Culleton, 2012) and Mexico (Culleton et al., 2015); but have yet to be applied to many South American shell middens.

We report here detailed geoarchaeological and chronostratigraphic investigations of La Yerba II, a large Middle Preceramic shell-matrix site on the estuary of the Río Ica, south coast of Peru. Bayesian modelling of 23 radiocarbon dates, micromorphology and other geoarchaeological analyses are used to understand the mound's formation. Alongside diverse other lines of archaeological evidence from La Yerba II's stratigraphy and modelling of changed coastline morphology at the time of its occupation, these offer new insights into changing marine hunter-gatherer lifestyles during a period critical to the transition to sedentism and the intensified exploitation of marine resources; the onset of modern El Niño Southern Oscillation (ENSO) conditions; and the formation of today's estuarine and beach habitats following the stabilisation of eustatic sea-levels: changes which foreshadowed the eventual emergence of monumental civilization along this Pacific coast during the subsequent Late Preceramic just before 5000 cal BP (Dillehay, 2017; Mauricio et al., 2021).

2. Materials & methods

2.1. Excavations in the La Yerba II shell midden

La Yerba II (or '15bVII 100' in Engel, 1981) is a large mound 175 m long by 86 m wide sitting atop a relict marine terrace overlooking a wave cut platform around 800 m from today's shoreline on the eastern bank of the Río Ica estuary, south coast Peru (see Fig. 2). The elevation of the relict terrace corresponds to the well-expressed MIS 5e terrace feature mapped along the Peruvian coast (Freisleben et al., 2021, Fig. 1).

The site was visited and mentioned by several pioneers of Peruvian archaeology including Max Uhle, Julio C. Tello and Alfred Kroeber (Kroeber et al., 1924; Casavilca Curaca, 1958; Lanning, 1967), and given various names over time.[1] Here we follow Frédéric Engel's (1991) nomenclature, since he was the first (and last) to excavate the site in 1956. La Yerba II's deposits cover some 9200 m^2 of the MIS 5e marine terrace to a maximum depth at its centre of over 4.5 m. The mound's highest surface lies 21.9 m above today's mean sea level (see Fig. 3). Some 75 m^2 of La Yerba II's southern extremity is overlain by some much later Middle Horizon

[1] La Yerba II has also been variously called: 'L-1' Cook (1994), 'Casavilca' (Lanning, 1967), 'CIZA 15bVII 100' (Engel, 1981), 'Morro La Gringa' (Carmichael and Cordy-Collins, 2020) and 'ICA-IN' (Carré et al., 2014).

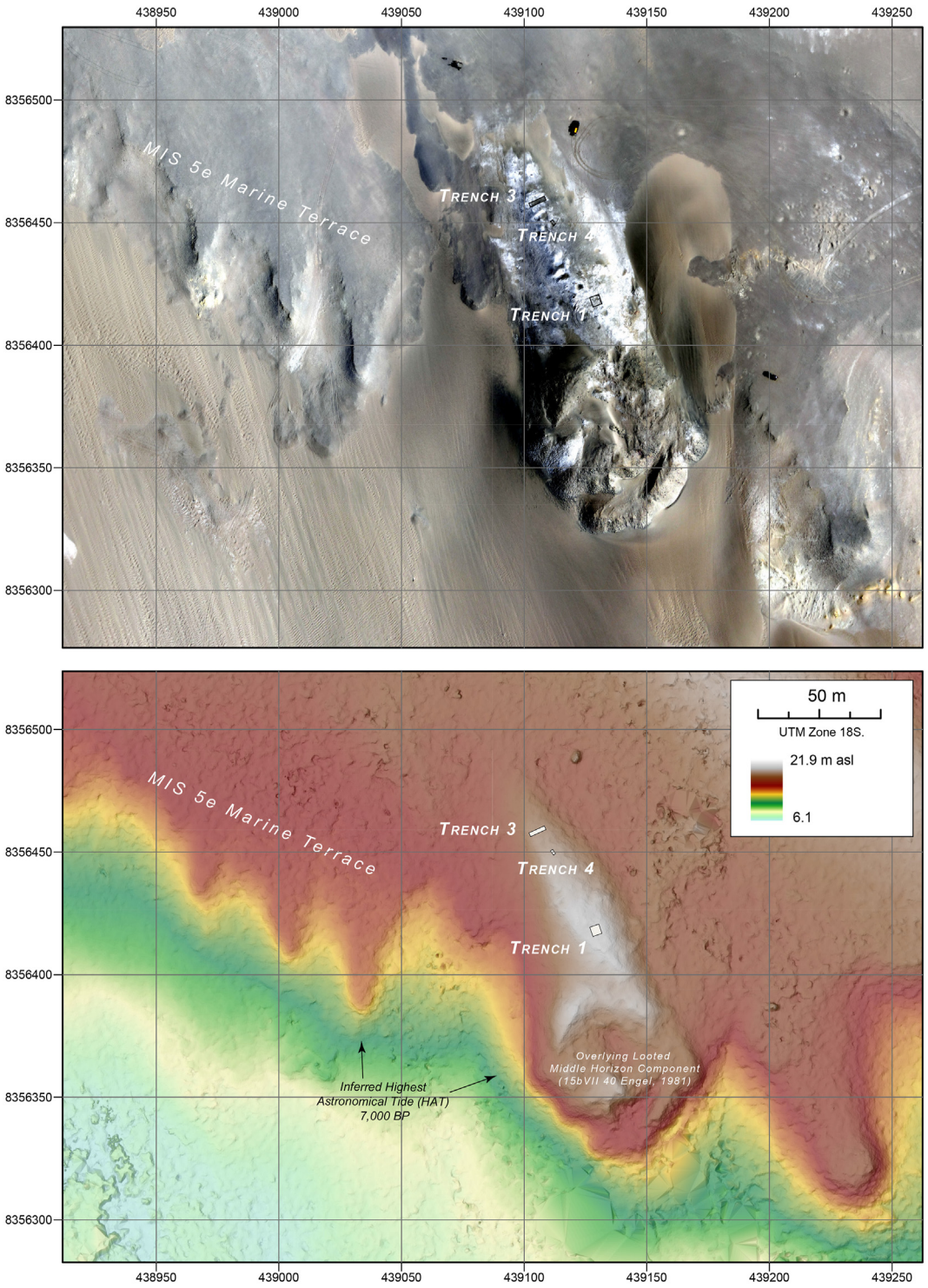

Fig. 3. Top: Orthographic aerial photograph, and Bottom: DEM of La Yerba II midden site showing the location of excavations, MiS 5e marine terrace and inferred HAT shoreline at 7 k BP.

(c. AD 1000 CE) deposits and remnants of adobe architecture, an area separately delineated by Engel as '15bVII 40' (Engel, 1981).

We carried out three excavations in La Yerba II discussed here (Arce et al., 2014):

1. A large trench (Trench 1) in the mound's central highest part at 21.9 m AMSL, excavated in steps (4 × 4 m at surface) to expose 4.4 m of stratigraphy without encountering the underlying natural marine terrace surface (see Fig. 4).
2. Re-excavation of presumed Engel 1956 trench (Trench 3, 4 × 1 m) at 20.32 m AMSL at the mound's northern extremity exposing 2.4 m of stratigraphy before reaching the natural marine terrace surface (see Fig. 5) (Engel, 1981).

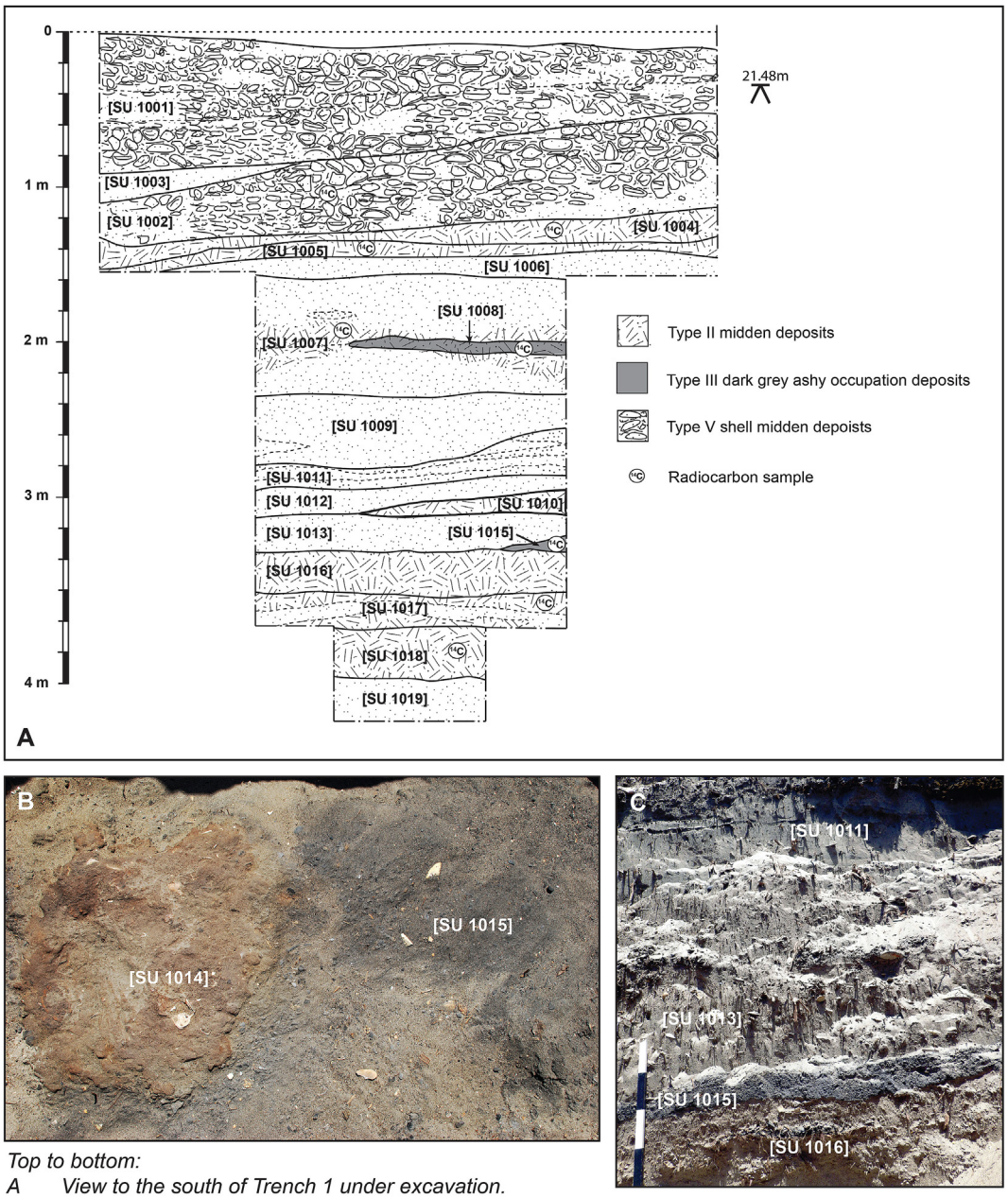

Top to bottom:
A View to the south of Trench 1 under excavation.
B Plan detail of Type IV brown, hard, indurated fine sediment deposit (SU 1014) lying immediately atop SU 1015.
C Section detail of Type III ashy occupation deposit (SU 1015) in Trench 1 NE-facing section.

Fig. 4. Details of Trench 1 excavation and southeast-facing section, La Yerba II.

3. Re-excavation of Carré's 2007 palaeoclimatic research trench (Trench 4, 1 × 1 m) at 20.83 m AMSL (see Fig. 6) (Carré, personal communication).

Excavation followed the British convention of determining stratigraphic units and recording archaeological sediments, natural layers, lenses, finds and other elements according to those units (MOLAS, 1994). Datum points, excavation positions and the depths of all contexts were established using a Leica 1200 differential global navigation satellite system (GNSS) and Nikon DTM 322 Total Station (see survey methodology below). All excavated deposits were screened on site through a 5 mm calibrated mesh sieve and measured 12L samples of all stratigraphic contexts taken for flotation screening (1 mm and 0.5 mm calibrated mesh) together to identify and quantify, *inter alia*, lithic, wood and plant fabric artefacts alongside marine and terrestrial mollusc, crustacean, fish, terrestrial and marine mammal and plant remains.

La Yerba II's contexts were characterised in the field according to five generalised interpretive groups, later refined by geo-archaeological analysis:

I. Unconsolidated, wind-blown sandy deposits with few cultural materials represented in Trench 1 by SU 1006, 1009, 1011, 1012 and 1019; in Trench 3 by SU 1055, 1056, 1058, 1059, 1076, 1077 and 1082; and in Trench 4 by SU 1061, 1062, 1070, 1066 and 1067.

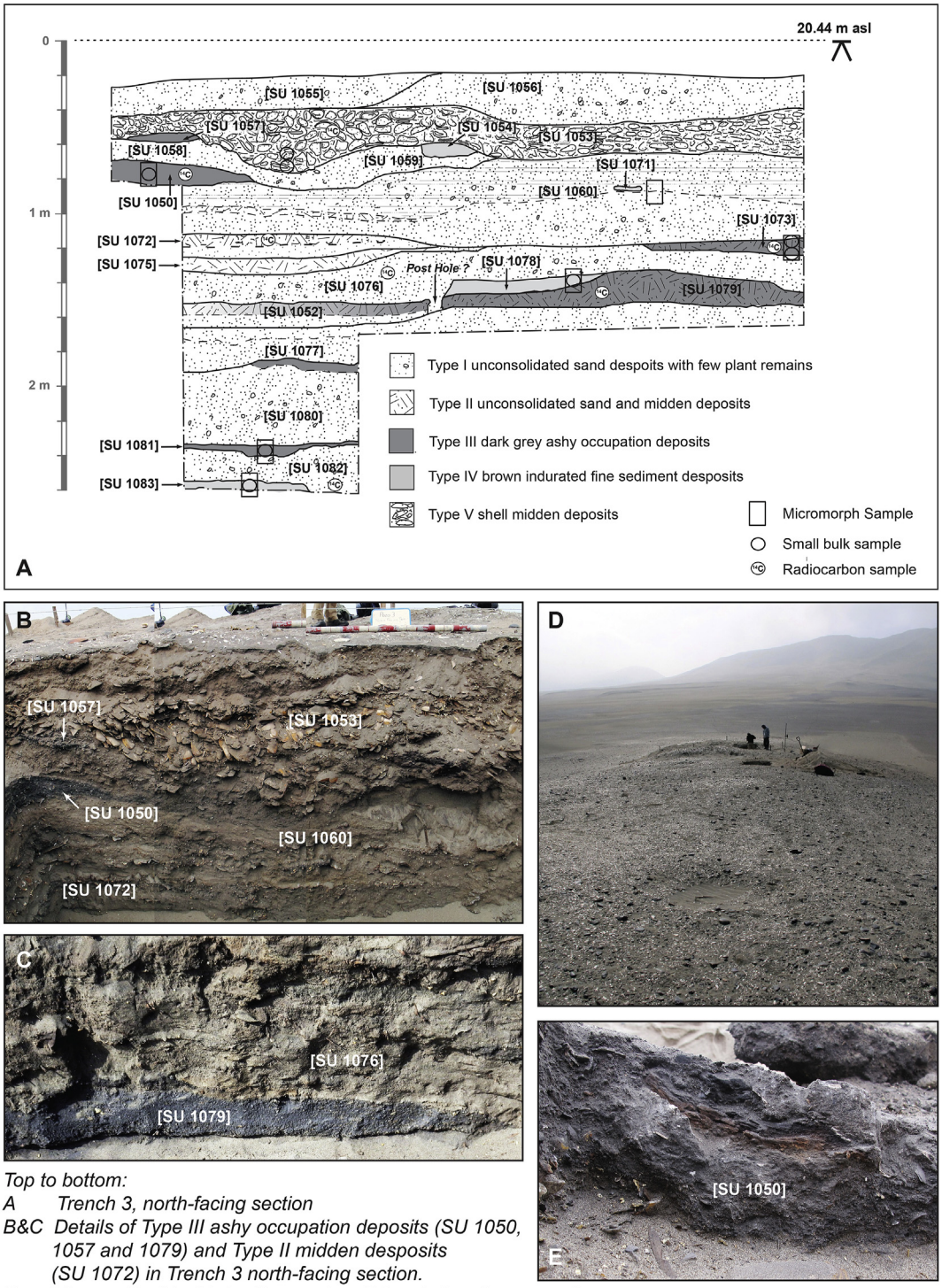

Top to bottom:
A Trench 3, north-facing section
B&C Details of Type III ashy occupation deposits (SU 1050, 1057 and 1079) and Type II midden desposits (SU 1072) in Trench 3 north-facing section.
D View north of La Yerba II mound and Trench 3 under excavation.
E Detail of consolidated ashy occupation deposit SU 1050 with inclusions of collapsed reed structure.

Fig. 5. Details of Trench 3 excavation and north-facing section, La Yerba II.

II. Unconsolidated sandy layers with varying concentrations of midden materials such as mollusc, crustacean, fish and plant remains and frequent lithic, fabric and shell artefacts, represented in Trench 1 by SU 1004, 1005, 1007, 1010, 1016, 1017 and 1018; in Trench 3 by SU 1072, 1075 and 1052; and in Trench 4 by SU 1060, 1063 and 1069. These are frequently stratigraphically associated with (or grade into) the ashier deposits of Type III below (e.g. in Trench 1 SU 1007 and 1008, see Fig. 4A; and in Trench 3 SU 1052 & 1079; and SU 1075 & 1073, see Fig. 5A).

III. Stratigraphically well-defined, well to poorly consolidated, grey ashy-sand layers that generally end abruptly rather than lensing out, with frequent, fragmented plant remains, crustaceans and molluscs, represented in Trench 1 by SU 1008

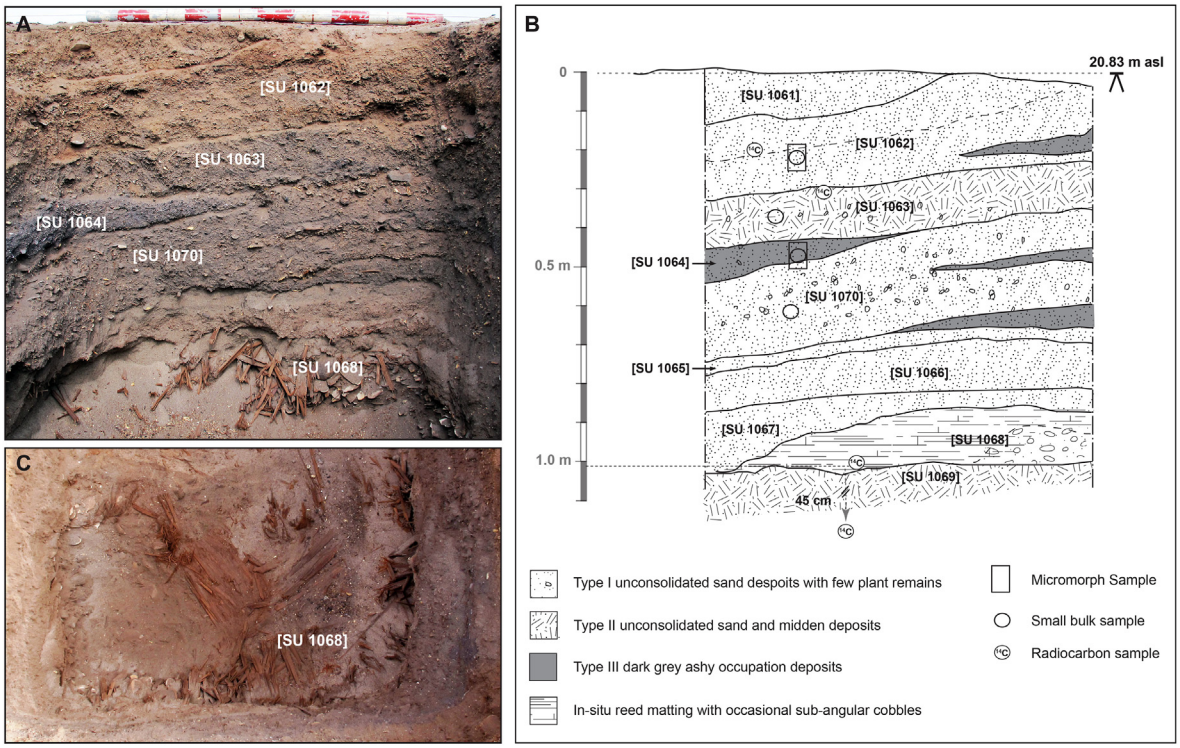

Top to bottom:
A&B Trench 4, north-facing section highlighting Type III ashy occupation deposits (SU 1064),Type II midden desposits (SU 1063) and in-situ collapsed reed structure (SU 1068).
C Plan detail of Trench 4 in-situ collapsed reed structure (SU 1068).

Fig. 6. Details of Trench 4 excavation and north-facing section, La Yerba II.

and 1015, in Trench 3 by SU 1050, 1051, 1057, 1073, 1079 and 1081 and in Trench 4 by SU 1064 and lenses in SU 1062 and 1070.

IV. Stratigraphically well-defined and in plan roughly circular deposits of brown, hard, indurated fine sediment with inclusions of highly fragmented midden materials, represented in Trench 1 by SU 1014 and in Trench 3 by SU 1071, 1054, 1078 and 1083. These relatively scarce deposits lie in immediate stratigraphic association atop of deposits of Type III above (e.g. in Trench 1, SU 1014 on top of SU 1015; and in Trench 3, SU 1078 atop 1079, see Figs. 4C and 5A).

V. Thick upper context layers of shell midden *sensu stricto* (Waselkov, 1987), dominated by surf clams (*Mesodesma donacium*), represented in Trench 1 by SU 1001 and 1002 and in Trench 3 by SU 1053.

Table 1 summarises these field descriptions for the deposits selected for geoarchaeological analyses while detailed field descriptions of all La Yerba II stratigraphic units are given in Supplementary Information.

2.2. Survey

A pedestrian survey was carried out using real time kinematic (RTK) global navigation satellite system (GNSS) to gather data on the La Yerba II mound and the key geomorphological features of its surrounding Rio Ica estuary landscape, as well as to provide elevation data and locate ground control points for aerial survey. A senseFly ebee drone was used to capture aerial photographs, which in turn were processed into an orthomosaic and digital elevation models within agisoft metashape. Together this allowed for detailed mapping of key features at high (centrimetric) resolutions. Additional, regional elevation data was extracted from AW3D, provided by the Japan Aerospace Exploration Agency, with wider photographic imagery drawn from sentinel two and airbus via the UP4 service. Elevations for features such as the exposed terraces were then compared to regional datasets (e.g. Freisleben et al., 2021), and imported into ArcGIS pro to check conformity to known and dated sequences.

For more details of these methods see Supplementary Information.

2.3. Radiocarbon dating

23 samples were selected for radiocarbon dating from 21 stratigraphic contexts: 14 from Trench 1 and 7 from Trench 3 (see Table 2, Figs. 4D and 5A). Hyper-arid conditions preserve a wide array of suitable organic remains. Only terrestrial plant materials were dated to avoid potential reservoir effects in a region with strong marine upwelling. These were mostly of short-lived plant species: desiccated or carbonised Cyperaceae rhizomes gathered for use as food or fuel, *Phragmites* sp. reeds used in shelter construction, organic artefacts in the form of yarns spun from plant bast fibre (*Asclepias* spp. *or Funastrum* sp., see Beresford-Jones et al., 2018) and fragments of bottle gourd (*Lagenaria* sp.). Three contexts were dated using wood charcoals with strong ring curvature suggesting that they originated from small branches.

AMS radiocarbon dating was carried out by the Oxford University Radiocarbon Accelerator Unit, following Bronk Ramsey et al., 2002, Bronk Ramsey et al., 2004. Of 23 samples submitted, one from SU 1001 the midden's surface context yielded a modern date and one from Trench 3, SU 1082 failed due to low yield. The La

Yerba II midden chronology is thus defined by 14 new radiocarbon dates from 13 stratigraphic units of Trench 1 and 7 new radiocarbon dates from 7 stratigraphic units of Trench 3, alongside four previously published dates (Carré et al., 2012: Table 1 'Rio Ica site') from Trench 4's stratigraphy (Fig. 6B, Carré, personal communication). These were all calibrated using ShCal20 (Hogg et al., 2020) and then modelled using OxCal v 4.4.4's Bayesian analysis (following Bronk Ramsey, 2009) as a sequence of phases to define boundary limits for the midden's chronology (see Table 2, Fig. 7).

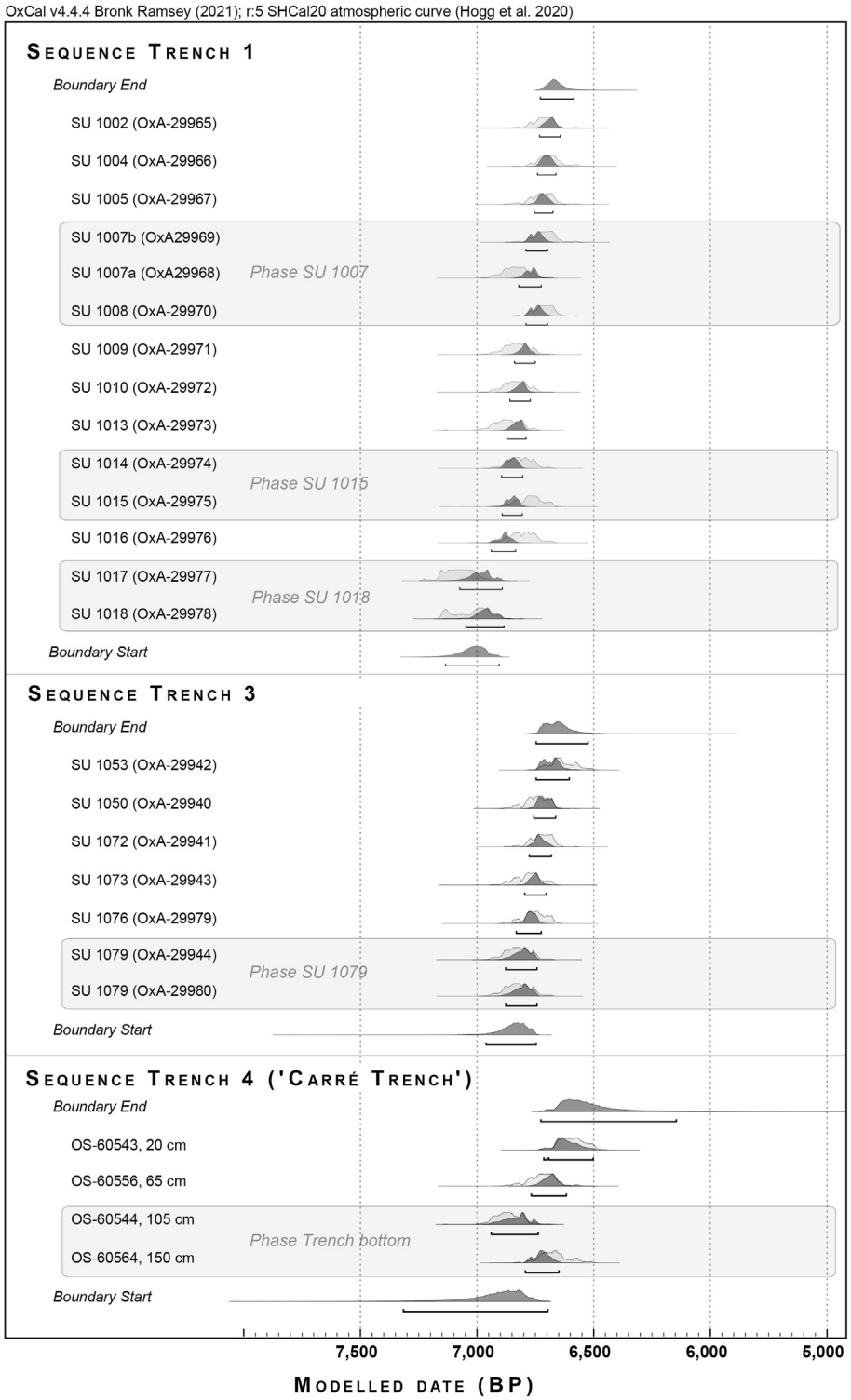

Fig. 7. Radiocarbon dates from La Yerba II calibrated using ShCal20 (Hogg et al., 2020) and modelled using Ox Cal v 4.3's Bayesian analysis (Bronk Ramsey, 2009) as a sequence of phases.

2.4. Geoarchaeological analyses

Geoarchaeological samples were targeted on contexts interpreted in the field to represent occupation surfaces and deposits of Types II, III and IV described above, which were encountered between relatively thicker blown sand and shell midden deposits of Type I and V, respectively, throughout the profiles of all excavated trenches (see Table 1). Nine undisturbed monolith sediment blocks were taken from stratigraphic contexts in exposed sections of Trenches 3 and 4 along with complementary small bulk samples (see Figs. 5A and 6B). To provide wider geomorphological background context six block samples were also taken from an inset terrace in the Río Ica estuary floodplain adjacent to La Yerba II and from the southern floodplain margin of the Río Ica around 1 km upstream from the site and the river's mouth (Profiles 20, 14 and 15, respectively). Thin sections were prepared from these monoliths for microscopic examination and description. Bulk sediment samples from selected stratigraphic contexts were analysed for pH and magnetic susceptibility (MS); using Fourier-Transform Infrared (FTIR) spectroscopy to identify their mineral and organic components; and using Inductively Coupled Plasma-Atomic Emission Spectrometry (ICP-AES) to identify their principal elemental components, at the McBurney Laboratory, Cambridge and the ALS Laboratory Group, Seville, Spain, respectively.

For more details of these methods and analyses see Supplementary Information.

3. Results

3.1. Chronology

Table 2 shows La Yerba II modelled using OxCal's Bayesian analysis to test the coherence of their presumed stratigraphic associations. 14 new radiocarbon dates from Trench 1 are modelled as a sequence according to their stratigraphic position, with three phases within that sequence comprising of dates in equivalent stratigraphic positions (see Table 2). Seven new radiocarbon dates from Trench 3 are modelled as a sequence according to their stratigraphic position, with one phase for two dates from SU 1079 (see Fig. 7). Four dates previously published by Carré et al. (2012) for Trench 4 are modelled as a sequence according to their stratigraphic position with one phase for the base of the trench. Modelled, overall agreement indices ('A') of 78.5%, 135.3% and 99.9% confirm the integrity of the presumed stratigraphic associations for Trenches 1, 3 and 4, respectively (each being >60%). Median boundary dates for these modelled sequences are 6672–7011 cal BP, 6670–6845 cal BP and 6561–6903 cal BP for Trenches 1, 3 and 4, respectively: together providing a consistent and coherent chronological framework for the La Yerba II midden.

3.2. Malacology and other Zooarchaeology

In addition to fish and terrestrial plant remains reported elsewhere (Arce et al., 2014; Beresford-Jones et al., 2015, 2018), marine and terrestrial mollusc, crustacean, and terrestrial and marine mammal remains from systematic 12 L sampling of La Yerba II contexts were identified and quantified (see Fig. 8, and Supplemental Information, Tables S1 and S2).

3.3. Geoarchaeology

The results of geoarchaeological analyses of La Yerba II stratigraphic units are shown in Table 3 (FTIR analyses), Table 4 (pH, MS and multi-element analyses) and Table 5 (micromorphological analyses), and in Figs. 9 and 10. Detailed micromorphological descriptions of the contexts analysed are given in Supplemental Information.

4. Discussion

4.1. Site formation and stratigraphy

The natural and anthropogenic processes that formed the La Yerba II mound and the patterns of human behaviour that lay behind that formation some seven millennia ago at the mouth of the Río Ica can be discriminated by relating macroscopic characterisations of contexts made in the field with the results of microscopic geoarchaeological and geochemical analyses. In doing so we draw attention to similarities (and differences) with microscopic fabrics (or micro-facies, cf. Courty, 2001) noted other shell midden contexts, including those of Tierra del Fuego and Brazil reviewed by Villagran (2019), Mexico (Neff et al., 2015), and South Africa (Karkanas et al., 2015).

4.1.1. Type I and V unconsolidated sand horizons – Fabric 1

Unconsolidated sandy contexts characterised macroscopically as Type I and V are both defined microscopically by Fabric 1, distinguished by wind-blown material with high abundance of shells and shell fragments. Geochemical analyses show that the major mineral component of these contexts is quartz with only minor clay contributions (see Table 3). They show low levels of elements indicative of human activity such as phosphorus (a proxy for phosphate) and have highly alkaline pH levels (>8). Micromorphologically, Fabric 1 exhibits fine to very fine quartz sand deposits and abundant, fine to very fine sand-sized, micro-charcoal fragments (see Fig. 9A, Tables 5 and 6). The size range and shapes of the sand fraction is neither uniform nor well-sorted, suggesting that it probably originated from only a short distance away as wind-derived fine sediment from the nearby foreshore dunes, along with very fine charcoal probably also blown in from hearths in the immediate vicinity.

Type I contexts characterised by Fabric 1 are thus interpreted to represent episodic periods of abandonment and also surfaces on the periphery of shifting occupations. Type V contexts – horizons of shell midden *sensu stricto* — are also characterised by Fabric 1, distinguished only by their much greater proportion of shells. These fabrics are most comparable to micro-facies Type 3 associated with tossing of discarded shells in Fuegian middens (Villagran, 2019: 357), but without the predominant and often micro-laminar, very fine to fine sand components observed in La Yerba II's Fabric 1.

4.1.2. Type II unconsolidated midden deposits – Fabric 2

Unconsolidated sandy layers without significant ash components but with varying concentrations of midden materials characterised macroscopically as Type II are defined microscopically by Fabric 2, distinguished by mixtures of wind-blown quartz sand and brownish-blackish sediments. While quartz dominates the mineral assemblage of Fabric 2 contexts, they are also comprised of humified organic matter and clay (see Tables 3 and 5). They show relatively low levels of elements indicative of human activity and only weakly alkaline to circum-neutral pH's of between 6.3 and 7.5, perhaps due to degradation of their organic components (see Tables 4 and 6). Micromorphologically, Fabric 2 exhibits a mixture of fine to very fine quartz sand and yellowish brown, generally non-birefringent, silty clays, with fine charcoal and humified organic matter inclusions, occasionally exhibiting lensing (see Fig. 9B and C, Tables 5 and 6). These characteristics suggest that it is composed of a mixture of wind-blown sands and fine soil material which is probably silty clay alluvium from the adjacent Río Ica floodplain, combined with episodic organic midden accumulations.

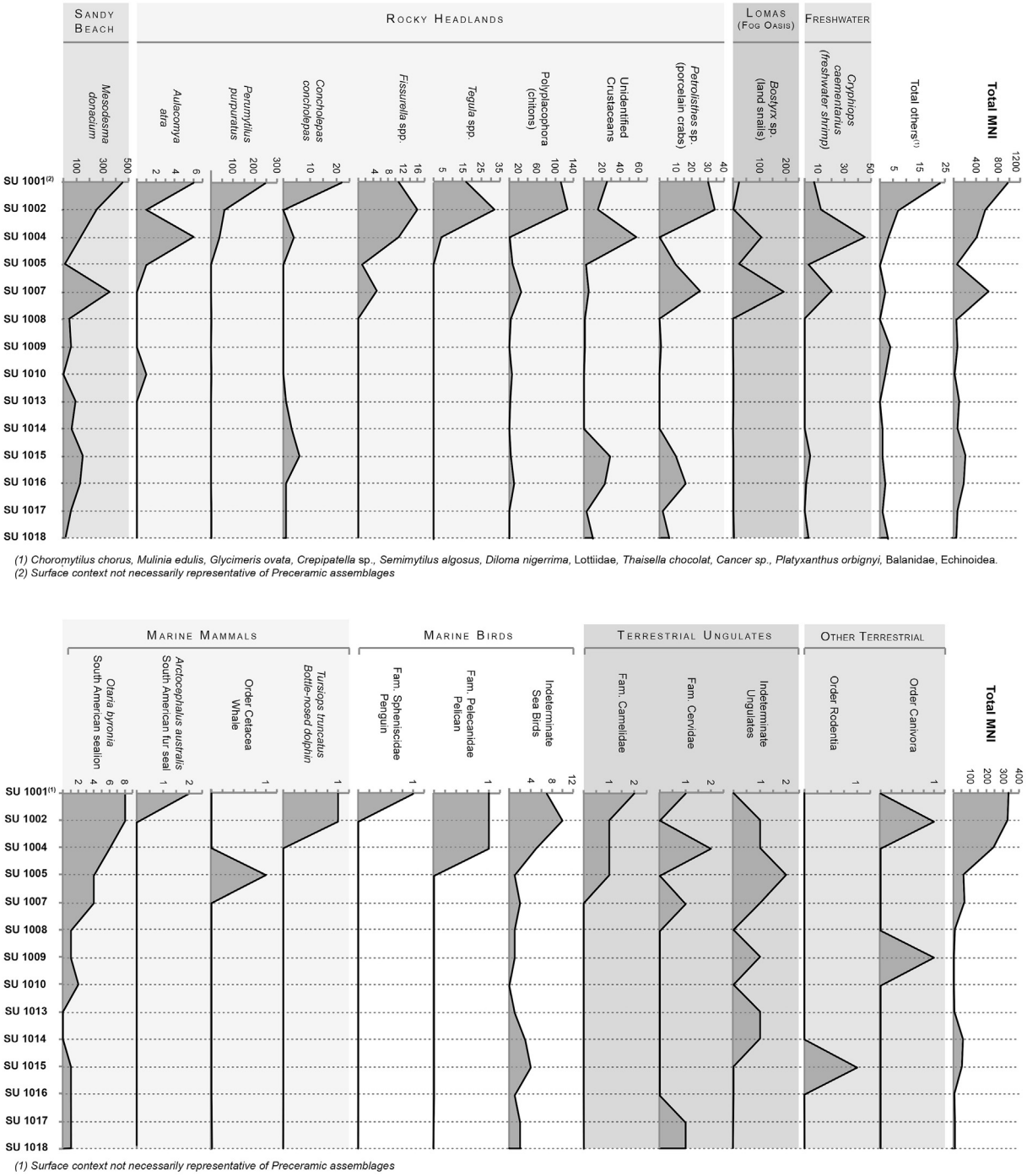

Fig. 8. Frequencies of malacological and other zooarchaeological remains in systematic sampling of La Yerba II, Trench 1 contexts by minimum number of individuals (MNI).

Type II contexts characterised by Fabric 2 are interpreted to represent areas of rubbish discard and associated dune accumulation on the periphery of shifting occupations. This fabric is comparable to micro-facies Type A in Brazilian shell mounds, deemed to represent multiple residues with a preponderance of shells (Villagran, 2019: 365–6).

4.1.3. Type III ashy deposits – Fabric 3

Stratigraphically well-defined, grey ashy layers characterised macroscopically as Type III are defined microscopically by Fabric 3. These ashy, charcoal-rich deposits show varying degrees of cementation. Some terminate abruptly in profile rather than lensing out and show possible vestiges of post-holes (e.g. SU 1079, Fig. 5A), or contain flattened plant remains (e.g. SU 1050, Fig. 10C).

Fabric 3 is composed of a dark grey to black sediments in the form of horizontal but discontinuous lenses and occasionally thicker horizons of very fine sand mixed with abundant very fine to fine charcoal and organic midden materials. Micromorphologically these dark grey and blackish deposits are associated with fine to coarse charcoal-rich, 'ashy', organic fine sandy lenses (Figs. 9D and 10C, Tables 5 and 6). Fabric 3 deposits have the highest pH values of all La Yerba II contexts (8–9) and contain high amounts of silt-sized

Table 3
Results of Fourier-transform infrared spectroscopy analyses of La Yerba II contexts.

Context	Sample No.	Fabric(s)	Description	Major Mineral Components Q = quartz; Cl = clay; Ca = calcite; A = aragonite; CAHP = carbonated hydroxylapatite; org = organic matter
TRENCH 3				
SU 1050	395	3 & 4	Blackish sediment with sand and white pieces White pieces	Cl, Q > Ca Ca
SU 1073/1	423	3	Blackish sediment with sand and small greyish pieces Grey flat piece	Q > Ca Ca
SU 1073/2	424	3	Blackish sediment with sand, charcoal and grey flat pieces Grey flat piece	Ca > Q, Cl > CHAP Ca
SU 1078	397	4 over 3	Blackish sediment with sand and small yellowish pieces Yellowish piece	Q, Cl, org Org
SU 1081	384	3	Black sediment with plant remains and sand White flat piece	Ca > Q, Cl A
SU 1083	389	3 & 5	Blackish sediment with chert, sand and white pieces White piece	CHAP > Ca CHAP
TRENCH 4 ('Carré Trench')				
SU 1062	412	2 & 5	Blackish sediment with sand and small yellowish pieces Yellowish piece	Cl, Q > Ca Ca > Q
SU 1062 (24-26 cm)	416	2 & 5	Blackish-yellowish sediment with sand and small yellowish pieces	Q, Cl
SU 1063	410	2 & 3	Blackish sediment with sand (Q, Cl) and small yellowish pieces Yellowish piece	Q, Cl org > Ca
SU 1063 (35-37 cm)	418	4	Blackish-yellowish sediment with charcoal, sand and small yellowish pieces	Q > Cl > CHAP, Ca, org
SU 1064	417	4	Blackish-yellowish sediment with sand and small yellowish pieces	Q, Cl, Ca
SU 1064 (46-48 cm)	414	3	Blackish sediment with sand and small bright white grains	Q > Cl > CHAP, Ca, org
SU 1070	413	3	Blackish sediment with sand and small yellowish pieces Yellowish piece	Q > Cl > Ca Ca > Cl, Q
SU 1068 (82-5 cm)	415	5	Greyish- blackish sediment with sand and small bright white grains	Q > Cl > CHAP, Ca, org

Table 4
Results of geochemical analyses of La Yerba II contexts.

Context	Sample No.	Fabric(s)	pH	MagSus SI/g	Ba (ppm)	Ca (%)	Cu (ppm)	Fe (%)	K (%)	Mg (%)	Mn (ppm)	Na (%)	P (ppm)	*Sr (ppm)*	*Zn (ppm)*
TRENCH 3															
SU 1053 (68–75 cm)	401	1	7.7	3.68	160	1.48	111	3.98	0.51	1.32	738	1.15	1130	130	114
SU 1053 (75–84 cm)	400	1	8.2	2.51	120	1.08	97	4.18	0.47	1.2	605	0.75	1130	95	108
SU 1050	395	3 & 4	8.8	5.85	40	3.67	13	2.42	0.98	1.13	283	3.84	3520	906	45
SU 1073/1	423	3	7.9	3.79	20	4.49	12	0.93	2.08	0.77	147	7.05	3140	390	32
SU 1073/2	424	3	8.6	2.38	20	4.71	13	1.17	0.86	0.68	173	2.0	4170	486	35
SU 1078	397	4 over 3	6.3	1.52	20	0.99	7	0.91	0.2	0.3	119	0.37	1910	85	290
SU 1081	384	3	9.0	9.86	120	7.31	20	0.72	0.22	1.05	135	>10	>10000	727	79
SU 1083	389	3 & 5	8.0	2.38	30	1.25	8	2.48	2.97	0.65	195	3.12	2590	308	30
TRENCH 4 ('Carré Trench')															
SU 1062	412	2 & 5	7.1	3.95	20	1.75	13	1.58	0.41	0.46	162	1.29	2890	166	39
SU 1062 (24-26 cm)	416	2 & 5	7.5	1.86	20	1.9	12	1.57	0.63	0.55	166	1.75	3070	183	39
SU 1063	410	3	7.3	2.97	20	1.79	13	1.61	0.44	0.45	194	1.12	2510	156	38
SU 1063 (35-37 cm)	418	3	7.5	n/a	20	1.59	11	1.65	0.45	0.41	183	1.22	2310	134	33
SU 1064	417	3	9.0	2.98	20	2.22	12	1.43	0.47	0.46	199	1.01	2730	229	33
SU 1064 (46-48 cm)	414	3	9.2	2.5	20	2.61	12	1.48	0.56	0.49	203	1.15	3170	268	35
SU 1070	413	3	7.4	2.6	20	1.16	10	1.41	0.25	0.37	162	0.58	1720	89	28
SU 1068 (82-5 cm)	415	5	7.8	2.33	10	0.69	8	1.24	0.15	0.32	139	0.44		41	22

calcite, some of which is calcitic ash (see Table 4). While some (e.g. SU 1073, see Tables 3 and 6) contain shell fragments composed of calcite and are enriched mainly in Ca, others (e.g. SU 1081) contain fragments of aragonite and significant levels of Ba, Ca, P, Na and Sr. Fabric 3 deposits have relatively high magnetic susceptibilities (SU 1081 with a value of 9.86 SI, the highest analysed, see Table 4) – suggesting that the integrity of their ashy content was quite quickly buried and protected by constantly aggrading wind-blown sands evident throughout the La Yerba II stratigraphic complex (cf. Allen and Macphail, 1987). Some Fabric 3 ashy deposits are cemented with micritic calcium carbonate, suggesting diagenetic alterations by exposure to sea spray from a proximate surf line (Cooke et al., 1993: 34; McLaren, 1995).

Type III ashy deposits characterised by Fabric 3 are interpreted to represent the interiors of wind-shelter constructions. These deposits have no direct correlation with micro-facies in Fuegian or Brazilian shell middens (Villagran, 2019).

4.1.4. *Type IV indurated fine sediment living surfaces – fabrics 4 & 5*

Stratigraphically well-defined deposits of brown, hard, indurated fine sediment characterised macroscopically in the field as Type IV were further refined by geochemical and micromorphological analyses into two distinct fabrics:

Fabric 4 is composed mainly of clay and quartz with some calcite and organic matter (see Table 3). Its pH levels are very alkaline at 7.5–8.8, and values of elements indicative of human activity are

Table 5
Summary of micromorphological thin section descriptions of La Yerba II contexts.

Context	Fabric(s)	Main fabric	Inclusions	Interpretation
TRENCH 3 ('Engel Trench')				
SU 1050	3 & 5	Finely laminar dark grey micritic fine to very fine sand	Abundant fine charcoal and common shell and bone fragments and silicified and humified plant tissue organic matter, often replaced with amorphous ssequioxides; common micrite and amorphous calcium carbonate throughout, and irregular zones of calcitic ash	Discrete zone of repeated accumulations of wind-blown very fine to fine sand and abundant midden debris which is bioturbated, disturbed and affected by secondary cementation with calcium carbonate
SU 1060	1 lenses & 4 surface in 2	Two intermixed fabrics in irregular aggregates/zones, with weakly defined horizontal orientation; predominantly (60–70%) pale yellowish brown to golden brown silty clay, intermixed with a very fine quartz sand with a minor (30–40%) silty clay component and common degraded bone fragments; becomes more porous and affected by amorphous calcium carbonate infills of the void space down-profile	At 13 cm down the context (at c. 81–82 cm depth) there is a distinct horizontal lens of humified organic matter situated above a *c.* 8–10 mm thick zone of a dense, humic, very fine sandy/silty clay fabric with evident fine horizontal/vertical cracks below and planar voids at its surface; otherwise much less organic than other sampled contexts	Combination of wind-blown very fine sand, midden debris and a silty clay fabric derived from elsewhere; with a series of superimposed, thin, but prepared floor surfaces at 81 cm down-profile, compacted through trampling and use (cf. Ge et al., 1993).
SU 1073/1 & SU 1073/2	3	Dark grey, porous, organic micritic fine sand	Common shell and bone, and frequent fine charcoal fragments	Discrete zone of bioturbated, fine charcoal-rich, midden debris with secondary cementation with calcium carbonate
SU 1078	4 over 3	An irregular mixture of two fabrics: a humic and amorphous iron stained fine quartz sand intermixed in irregular zones with an amorphous iron stained fine quartz sand with a few silty clay aggregates; over a fine quartz sand	Upper 5–5.5 cm with humic and amorphous iron staining, and common, sub-rounded silty clay aggregates, and common charcoal, bone and shell fragments; lower 4.5–5 cm with sub-rounded silty clay aggregates, and amorphous iron staining	Disturbed and mixed wind-blown sand, midden and silty clay material, possibly a former floor surface, overlying fine dune sand
SU 1081	3	As for 1073 above	As for 1073 above	As for 1073 above
SU 1083	3 & 5	Dark grey to brown mixture of fine sub-rounded pebbles and a porous fine to very fine micritic sand with a minor silty clay component	Frequent fragments of humified and pellety organic matter, fine charcoal, abundant degraded and weathered bone fragments and common shell fragments	Discrete zone of bioturbated living surface with abundant included midden debris, affected by subsequent surface weathering
TRENCH 4 ('Carré Trench')				
SU 1062	2	Thin zone of orangey-red amorphous iron and phosphatised sand over a brown humic, very fine to fine sand with finely aggregated silty clay, all stained with amorphous sesquioxides	Common fine charcoal, humified organic matter, degraded bone and shell fragments	Possible weathered surface with midden material at a possible stratigraphic break in the porous mix of weathered silty clay, midden material and fine beach sand, much affected by oxidation and secondary formation of iron oxides
SU 1064	3	Porous, aggregated to single grain, very humic, fine sand; with three slight fabric/colour changes at c. 50, 53 and 56 cm	Abundant fragments of charcoal, charred and humified organic matter and bone	Episodic accumulation of organic midden material and wind-blown fine beach sand
Off-site Contexts (Río ica Floodplain)				
Profile 15 Inset terrace in estuary floodplain adjacent to La Yerba III		Fine lenses of fine to coarse quartz sand over a sub-angular blocky ped sandy/silty clay	Few fine charcoal and humified plant tissue fragments.	Episodically transported and redeposited sandy river-bed material over aggraded alluvial floodplain fine material
Profile 14 Southern floodplain margin c. 1 km upstream from La Yerba II		Golden brown, micro-laminated and non-laminated silty clay intermixed with very fine to medium quartz sand	Common charcoal and humified plant tissue fragments	Episodic aggradation of overbank alluvial material
Profile 20 Southern floodplain margin c. 1 km upstream from La Yerba II		A pale golden brown calcitic silty clay with a few silt crusts	Fine charcoal and humified plant tissue fragments	Episodic aggradation of overbank alluvial material with periods of severe surface drying out

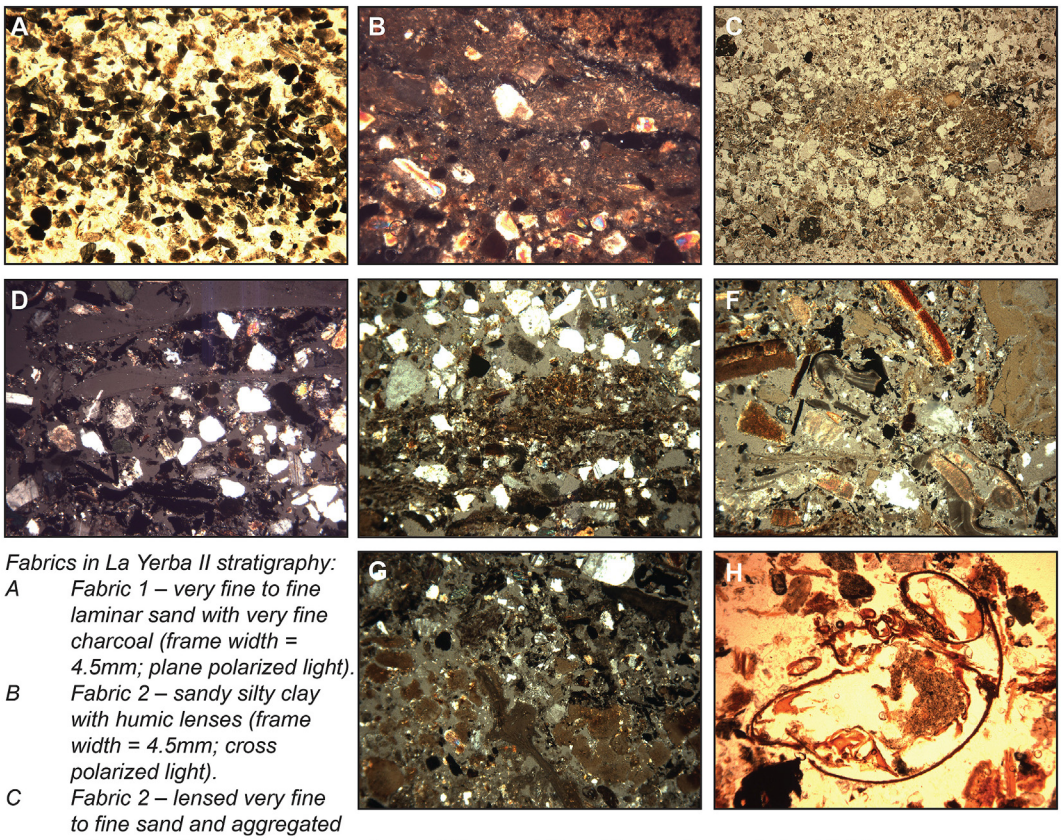

Fabrics in La Yerba II stratigraphy:

A Fabric 1 – very fine to fine laminar sand with very fine charcoal (frame width = 4.5mm; plane polarized light).

B Fabric 2 – sandy silty clay with humic lenses (frame width = 4.5mm; cross polarized light).

C Fabric 2 – lensed very fine to fine sand and aggregated silty clay with abundant micro-charcoal (frame width = 4.5mm; plane polarized light).

D Fabric 3 – very fine to fine sand, charcoal fragments and silicified plant tissues in vegetal voids (frame width = 4.5mm; cross polarized light).

E Fabric 4 – laminar humic material alternating with sand lenses (frame width = 4.5mm; cross polarized light).

F Fabric 4 – midden mix of sand, ash, bone, plant tissue, charcoal, shell and phosphatised bone (frame width = 4.5mm; cross polarized light).

G Fabric 5 – fragmentary phosphatised bone with charred and humified organic matter above (frame width = 4.5mm; cross polarized light).

H Fabric 5 – iron-phosphate-amorphous sesquioxide replaced and 'cemented' bone, shell and plant tissues (frame width = 4.5mm; plane polarized light).

Fig. 9. Photomicrographs of the five main fabric types in La Yerba II.

relatively low to medium (see Table 4). Micromorphologically this fabric is made up of thin, sometimes finely laminar, horizons of fine sand and/or fine pebbles with golden brown silty clays which appear identical to those described in micromorphological samples taken from the adjacent Río Ica floodplain (see Fig. 9E and Tables 5 and 6). These contexts often exhibit a heterogeneous mixture of highly fragmentary organic midden materials (see Fig. 9F). Their finely laminar and planar void aspects are suggestive of repeated applications and/or surface trampling (cf. Adderley et al., 2010; Ge et al., 1993; Karkanas et al., 2015). Deposits characterised by Fabric 4 (Fig. 10D, Tables 5 and 6) are interpreted to represent repeated episodes of surface preparation and use for particular short-lived purposes using sediments transported to the site from the adjacent river floodplain.

This fabric shares many features with micro-facies type 4 in Fuegian shell middens and micro-facies A1 in Brazilian shell mounds (Villigran, 2109: 364–5), including evidence of compaction, admixtures of clay or muddy sand (albeit from adjacent lagoonal areas in the latter rather than the alluvial material noted at La Yerba II) with common included micrite, organic matter, shell and bone. The fine laminar aspect of La Yerba II's Fabric 4 is, however, distinctive, perhaps reflecting Villigran's (2019, 366) suggestion of frequentation phases noted in Fuegian micro-facies type 6 and akin in other respects to La Yerba II's Fabric 5.

Fabric 5 is an indurated, pebbly fine sand sediment with fragmentary midden material, mainly degraded and phosphatised bone material. FTIR analysis shows these sediments to contain carbonated hydroxylapatite, alongside calcite, clay and quartz (see Table 3). Bone fragments in these contexts show a splitting factor of 5.6 suggesting that they were exposed to significant surface weathering (Weiner, 2010). This fabric shows high pH levels of around 8 and, like Fabric 4, relatively low values of magnetic susceptibility and the indicative set of elements for human activity (see Table 4). Micromorphologically, Fabric 5 shows a very porous mixture of fine sub-rounded pebbles and micritic very fine quartz sand with frequent pellety (or excremental) humified organic matter, fine charcoal, degraded phosphatised and sometimes burnt, bone materials and shell fragments (see Fig. 3, SU 1083; Fig. 9G and H, Tables 5 and 6); all 'cemented' with a combination of silty clay, secondary amorphous sesquioxides and micritic calcium carbonate. The relatively high amounts of carbonated hydroxylapatite and the general re-precipitation of secondary calcite throughout these

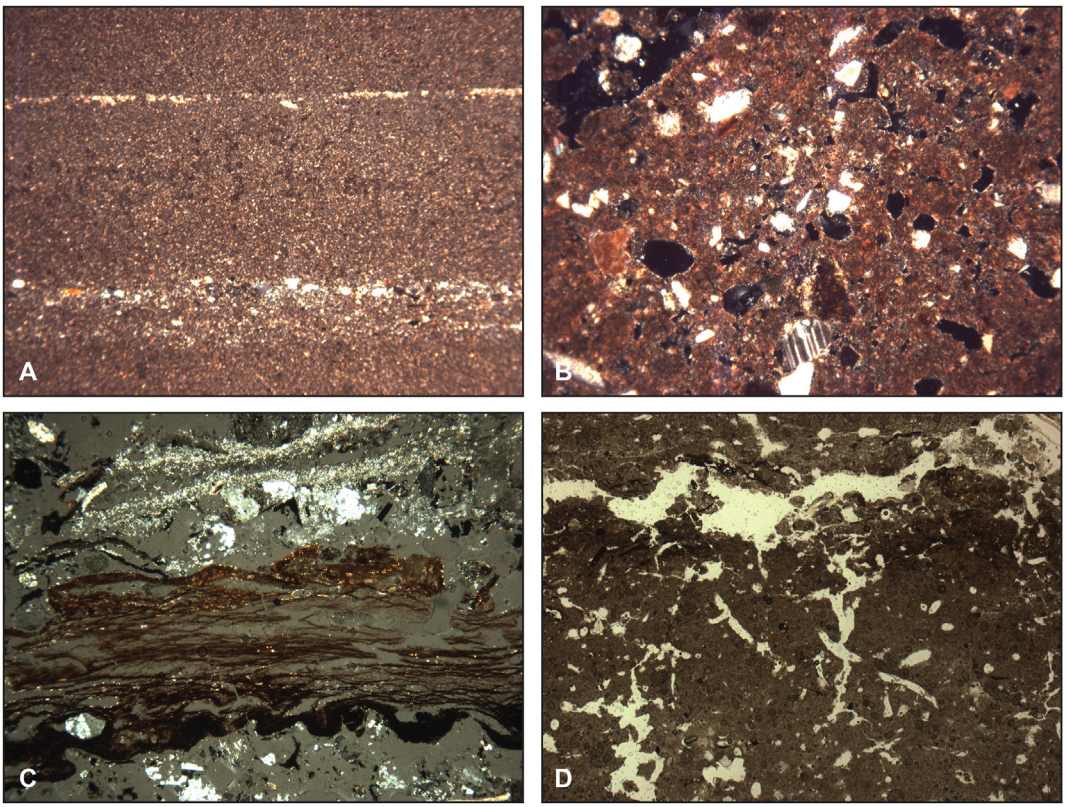

Photomicrographs of:

A *Modern Río Ica floodplain adjacent to La Yerba II Profile 1, Sample 404 – laminar silt and very fine sand deposits (frame width = 4.5mm; cross polarized light).*

B *Modern Río Ica floodplain, Profile 2, Sample 19 – vughy, humic and calcitic, sandy/silty clay (frame width = 4.5mm; cross polarized light).*

C *La Yerba II, Trench 3, SU 1050 – lensed calcitic ash over amorphous iron oxide replaced plant tissue over charred plant matter over a mixture of fine sand and ash (frame width = 4.5mm; cross polarized light).*

D *La Yerba II, Trench 3, SU 1060 – possible surface at c. 81-82cm of humic silty clay with planar voids at the upper surface and a fine crack structure below (plane polarized light; frame width = 1.5cm).*

Fig. 10. Photomicrographs of associated contexts.

sediments suggests decay of a high amount of organic remains on these surfaces alongside their sometime diagenetic alternations through exposure to sea spray (McLaren, 1995; Weiner, 2010). Fabric 5's pellety structure associated with humified organic materials may represent the weathered, exposed and bioturbated organic remains of collapsed wind-shelter constructions (cf. Friesem et al., 2014, 2016), elsewhere also well-preserved in the La Yerba II excavations (see Fig. 6C).

This fabric shows similarities with micro-facies Type 6 in Fuegian shell middens (Villagran, 2019, 366), although La Yerba II's Fabric 5 is much more fine-pebbly in texture with abundant bone and charcoal fragments, with bone exhibiting much more weathering and degradation, including common phosphatisation. In contrast, secondary phosphatisation was observed the Brazilian shell mounds and interpreted to be the result of soft tissue decay of aquatic animals from lagoonal contexts, rather than bone weathering (ibid.). In La Yerba II, however, evidence of bone degradation is clear in thin section (Fig. 8G and H), and in FTIR evidence of carbonated hydroxylapatite (cf. Karkanas and Goldberg, 2010; and see above and Tables 2 and 7).

Areas of these indurated Fabric 5 surfaces exposed in plan (see Fig. 4B) in La Yerba II are relatively small and discrete (to 2 m in diameter), but they show geochemical and micromorphological similarities with contexts interpreted to be floors in other shell-matrix sites in Fuegian, Mexico and the South Shetland Islands of Antarctica (Morello et al., 2012; Neff et al., 2015; and Villagran et al., 2013, respectively). In Tierra del Fuego at Punta Santa Ana calcitic ash and charcoal lenses covered indurated surfaces, while on Engelfield Island discrete brown, indurated, sub-rounded surfaces were noted between shell midden dumps (Morello et al., 2012). At Livingstone Island, Antarctica (Villagran et al., 2013) and the Archaic Tlacuachero shell mound in Chiapas, Mexico (Voorhies, 2015; Neff et al., 2015), geochemical data indicate that living surfaces around hearths were indurated with hydroxylapatite. These are considered to have formed diagenetically: the surface forming as a calcite dominated trampled level receives ash from hearths, which then reacts in solution with phosphates arising from the degradation of plant matter and bone/shell and fish food remains to produce hydroxylapatite. Deposits of Fabric 5 in La Yerba II are likewise interpreted to be the residues of occupation composed of degraded organic materials on floor surfaces mixed with midden debris and, sometimes, the remains of collapses and decayed structures (cf. Friesem et al., 2014).

4.2. Reconstruction of human activities

All La Yerba II deposits are circum-neutral to highly alkaline with pH's between 6.3 and 9.5 (see Table 4), as one might expect

Table 6
Summary of the main fabric types in La Yerba II stratigraphy.

Fabric	Contexts			Field description	Geochemistry	Micromorphology	Interpretation
	Trench 1	Trench 3	Trench 4				
1	SU 1003 SU 1006 SU 1013 SU 1006 SU 1019	SU 1055 SU 1056 SU 1058 SU 1059 SU 1076 SU 1077 SU 1080 SU 1082	SU 1061 SU 1065	Wind-blown material with high abundance of shells	Mainly quartz and some clay; Low levels of pH, Mag Sus and no enrichment of anthropogenic elements	Fine to very fine quartz sand deposits	Natural wind-blown infilling. Abandonment/low intensity of activity
2	SU 1004 SU 1005 SU 1007 SU 1010 SU 1011 SU 1016 SU 1017 SU 1018	SU 1060 SU 1072 SU 1075 SU 1052	SU 1062 SU 1063 SU 1069	Mixture of wind-blown material with brownish-blackish sediment	Mainly quartz with some clay and organic matter; Very low pH (organic degradation); Low levels of Mag Sus and no enrichment of anthropogenic elements	Fine to very fine sand and yellowish brown alluvial silty clay, with humified organic matter inclusions	Mixture of organic midden accumulations with wind-blown sand and fine alluvial soil material
3	SU 1008 SU 1015	SU 1050 SU 1057 SU 1073 SU 1079 SU 1081	SU 1063 SU 1064 SU 1070	Horizontal but discontinuous lenses of dark grey to black sediment mixed with charcoal and organic material	High amounts of calcite with quartz and clay; Aragonite shells; High pH levels (8–9); Some contexts enriched with Ba, Ca, P, Na, Sr and high Mag Sus;	Fine to coarse charcoal-rich, 'ashy', organic fine sandy lenses	Hearth rake-out and/or dumps of hearth derived material and insides of areesh wind shelters with some quite consolidated, exposed surfaces
4	SU 1014	SU 1071 SU 1078		Laminar thin horizons of fine sand and/or fine pebbles with silty clay	Clay and quartz and some calcite and organic matter; Very high pH levels (9); Low levels of Mag Sus and no enrichment of anthropogenic elements	Laminar fine sand, and/or fine pebbles and/or imported riverbed-derived silty clay material with planar void	Prepared floor surfaces
5		SU 1083	SU 1062 SU 1068	Indurated, pebbly fine sand sediment with fragmentary shells and degraded bones	Carbonated hydroxylapatite alongside calcite, clay and quartz; High pH level (8); Low levels of Mag Sus and no enrichment of anthropogenic elements	A very porous mixture of fine sub-rounded pebbles and micritic very fine quartz sand with frequent pellety, humified organic matter, fine charcoal, degraded bone fragments, common shell fragments and cemented with a combination of silty clay, secondary amorphous sesquioxides and micritic calcium carbonate	Basal surface of the camp with occupation residues, including shells, burnt bones, organics and collapsed thatch structure

given the quantities of whole and fragmented mollusc and crustacean shell throughout many of its contexts. The mound's uppermost contexts comprise thick horizons of shell midden *sensu stricto*, characterised macroscopically as Type V, and likely the outcome of simple shell tossing activities. These probably contributed to the preservation of the mound's form through subsequent millennia. Yet the bulk of La Yerba II's underlying sedimentation is the outcome of sequences of occupation and anthropogenic activity punctuated by periods of abandonment, favouring the near-constant accumulation of wind-blown sands in an extremely windy shoreline environment. Based on the characterization of the different macroscopic contexts according to the microscopic fabrics described, we identify at least 13 such occupation sequences in the La Yerba II stratigraphy, some of which were likely parallel in time. Largely wind-blown dune-like deposits (Type I and II, Fabrics 1 and 2) comprise around 60 percent of the stratigraphy of Trenches 1 and 3, some likely representing periods of abandonment and others spatial shifts in occupation within the site (see Table 6, Fig. 11).

Between these layers of wind-blown sediment representing episodes of abandonment or significantly reduced intensity of activity on the edges of shifting occupation, the La Yerba II stratigraphy includes clear evidence for the use of fire in the form of concentrations of ash and fine charcoal-rich layers (Fabric 3), prepared surfaces (Fabric 4), 'indurated' organic residues (Fabric 5), and, rubbish middening (Fabric 2, and throughout Fabrics 3–5 in varying concentrations and degrees of fragmentation).

These middens offer copious evidence of the foods hunted and gathered by its inhabitants from cold-water marine and terrestrial habitats (Arce et al., 2014; Beresford-Jones et al., 2015, 2018). Most conspicuous, not least for reasons of differential preservation, are the shells of 21 species of gastropod and bivalve molluscs, and in particular large quantities of machas (surf clams, *Mesodesma donacium*), accounting for 53% by number and 81% by weight of all molluscs identified from systematic sampling of the 14 contexts of Trench 1 (see Fig. 8). Proliferating in dense beds in shallow waters along sandy beaches and resilient to overexploitation, machas

offered an ideal protein source, easily collected without significant risk by all members of society. These middens also contain bones from 15 fish species (Beresford-Jones et al., 2018), mostly larger line-caught species (64% by Minimum Number of Individuals, 'MNI'), including corvina (sea bass, *Cilus gilberti,* 44% by MNI) of an average of 4 kg and up to 9 kg in weight. Of smaller schooling fish the vast majority (25% of total fish remains by MNI) are lisa (mullet, *Mugil cephalus*), likely trapped in the nearby river estuary during their spawning there in summer. Marine mammal bones are represented, particularly sea lions (*Otaria flavescens*) hunted from colonies on rocky headlands, some bottle-nosed dolphin (*Tursiops truncates*) and, presumably scavenged, indeterminate whale species (see Fig. 8). Crustaceans including very large numbers of muy muy (Pacific mole crab, *Emerita analoga*) were gathered from the beach and freshwater crayfish (*Cryphiops caementarius*) trapped in the river estuary in summer. Echinoderms (sea urchins) and edible kelps (*Macrocystis* spp.) were gathered from rocky headlands. Marine and terrestrial birds were hunted, including pelicans (Fam. Pelecanidae) and penguins (*Spheniscus humboldti*). On land guanaco (*Lama guanicoe*), deer (*Odocoileus virginianus*) and vizcachas (*Lagidium viscacia)* were hunted in lomas and riverine oases. Terrestrial molluscs (land snails, *Bostryx* sp.) proliferate in the winter *lomas* fog-oases and comprise almost 25% of La Yerba II's total mollusc assemblage by number, albeit only 1% by weight (Beresford-Jones et al., 2015). The middens also include copious charred and desiccated remains of plants gathered as fuel, food and construction materials. Most conspicuous, particularly in Type III/ Fabric 3 contexts, are large numbers of mostly charred, but sometimes desiccated, edible rhizomes of estuarine *Cyperaceae esculentus* ('chufa'). Finally, La Yerba II's contexts also contain evidence of the lithic, shell and, thanks to preservation in arid conditions, fabric artefacts and technologies used to harvest these marine and terrestrial resources (see Beresford-Jones et al., 2018: Fig. 8), and the remains of mats and collapsed structures woven from *Typha* and Cyperaceae leaves and stems (see Fig. 6C).

Despite this abundant evidence for human activity, however, the magnetic susceptibility and concentrations of elements typically taken as proxies of human occupation (Friesem et al., 2016, 2017), such as phosphorus (a proxy for phosphate) are rather low through the La Yerba II contexts (see Table 4). This reflects continuous sedimentation and burial of ephemeral occupation surfaces through in-blowing sands reworked from foreshore dune systems. In micromorphological thin section, the bulk of La Yerba II settlement-derived material is highly comminuted and fragmented, suggesting rapid surface weathering and decay through humification, oxidation and biodegradation. Ocean breezes off cold seas persist here throughout the year here and strengthen diurnally as the desert hinterland warms to become very strong in the afternoon before dropping in the evening. Throughout the contexts of La Yerba II there is a consistent input of very fine-medium quartz sand, most of which is wind-blown, but not well-sorted, suggesting that the foreshore dunes from which it originated lay in close proximity to the site.

Magnetic susceptibility and elements indicative of human activity are, however, relatively enhanced in those parts of the La Yerba II stratigraphy that represent the vestiges of settlement (see

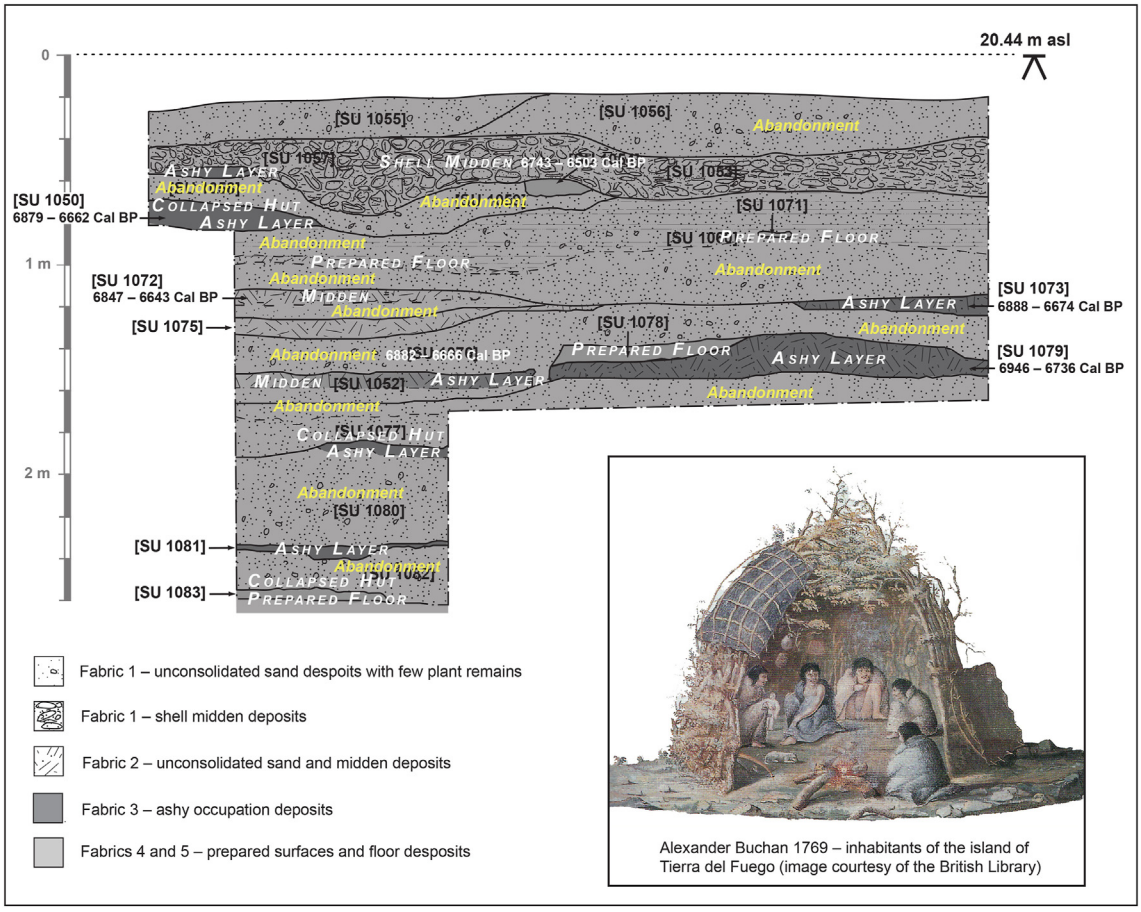

Fig. 11. Trench 3 stratigraphy showing sequences of occupation, human activities and dates.

Table 4). Ashy deposits of Fabric 3 and associated indurated floor and prepared surface deposits of Fabrics 4 and 5 have the highest phosphorus values, whereas unconsolidated sandy midden deposits of Fabrics 1 and 2 all have relatively low values. The ashy Fabric 3 deposit of SU 1081 towards the base of the La Yerba II stratigraphic sequence (see Fig. 5A) shows the highest magnetic susceptibility, alongside the very highest phosphorus accumulation and enhancement of barium and calcium: elements typically indicative of wood ash. Throughout La Yerba II's occupation deposits of Fabrics 3, 4 and 5, iron and manganese levels are weakly enhanced, yet the secondary formation of calcite is common (see Tables 3 and 4), helping to explain their consolidation and sometimes cementation into hard crusts. Varying degrees of cementation likely relate to differences in the scale and preservation of fire residues in the different contexts, varying oxidation and secondary formation of amorphous iron oxides and calcium carbonate, and varying exposure to sea-spray. All these micromorphological and geochemical patterns are compatible with occupation surfaces that were short-lived but nonetheless relatively longer-exposed and better sheltered from otherwise constantly aggrading wind-blown materials.

Human activity at La Yerba II clearly also involved the construction of surfaces and structures. Surfaces characterised by Fabric 4 seem to have been intentionally prepared from silty clay alluvium transported to the site from the nearby riverbed. Fabric 5, meanwhile, suggests an indurated surface with the sometime collapse of reed/thatch structural material above. Notably, indurated Fabric 5 deposits almost inevitably immediately overlie Fabric 3 ashy deposits (e.g. SU's 1014 and 1015 in Trench 1, and SU's 1078 and 1079 in Trench 3, see Figs. 4C and 5A), evidencing hearths and related ashy deposits and rake outs under structures (Fig. 11). Well-preserved woven reed (*Typha* sp.) matting in SU 1068, Trench 4 (see Fig. 5C) represents direct evidence of the type of architecture present on La Yerba II, akin to the *areesh*-type huts or wind-shelters described ethnographically (e.g. Lothrop, 1928) and archeologically (Estévez and Vila, 2006) for Yamana fisher hunter-gatherers in Tierra del Fuego. The well-defined and limited depths of ashy Fabric 3 accumulations suggest episodic wind shelter constructions in different locations within the site, among the earliest thus far identified in South America.

Taxonomic identification and analyses of ring curvature and radial cracking of La Yerba II charcoals suggest low temperature, small domestic fires fuelled with smaller, often green-wood, branches of woody shrubs (*Baccharis* and *Tessaria* spp.), willow (*Salix humboltiana*) and monocots (likely including rhizomes of estuarine *Cyperaceae* recovered both charred and desiccated in quantities from La Yerba II's contexts). Yet heavier woods of larger *Prosopis* and *Acacia* trees, presumably the dominant species of riverine dry forests heretofore undisturbed by agriculture, and which could have fuelled high temperature fires, are conspicuously absent from the La Yerba II charcoal assemblage. Such small, carefully controlled, fuel-thrifty domestic fires would be typical of hunter-gatherer groups. Aside from providing warmth and cooking, they could also have served to open bivalve molluscs such as surf clams efficiently in bulk (Waselkov, 1987), even if their contents were not then cooked. Indeed, the condition of La Yerba II midden remains alongside coprolite analysis from other Preceramic sites (Parsons, 1970) suggests that mussels, clams, crabs and sea urchins were often eaten raw: bringing some seven millennia of time depth to the tradition of *cebiche* in Peruvian cuisine.

In sum then, we interpret La Yerba II's stratigraphy to represent a palimpsest of the basecamps of logistically mobile (*sensu* Binford, 1980) complex marine hunter-gatherers. Their middens include copious evidence of resources hunted and gathered from nearby inshore marine pelagic habitats of the sandy beach and river estuary, but also from more distant marine benthic habitats and rocky headlands and the terrestrial habitats of riverine and ephemeral *lomas* winter fog oases. The logistical field camps and hunting stands from which many of these marine and terrestrial resources were targeted in rounds of seasonal mobility have been identified far along the littoral on seasonal fog-fed arroyo watercourses and deep within the lomas up to 25 km from La Yerba (Beresford-Jones et al., 2015, 2018). Obsidian lithics are relatively scarce in La Yerba II's Preceramic contexts but three flakes from Trench 1's SU 1007, 1010 and 1015 are defined by their geochemical fingerprints as having originated at the Jichja Parco quarry at Quispisisa over 170 km away in the Ayacucho highlands at 4,100m asl (Chauca et al., 2019). Yet, while some of La Yerba II's occupants were apparently highly mobile, the archaeological record presented here also reveals sometime intense occupation and considerable investment in site construction. The La Yerba II contexts are not merely the vestiges of simple shell-tossing activities, or some form of task-specific campsites. 21 radiocarbon dates from Trenches 1 and 3, and four previously published dates for Trench 4, provide a coherent chronological framework for these processes of site formation.

4.3. Chronostratigraphy

OxCal Bayesian modelling of these dates as a sequence of phases according to their stratigraphic sequence gives median boundary limits of between 6672 and 7011 cal BP for Trench 1; between 6670 and 6845 cal BP for Trench 3; and between 6561 and 6903 cal BP for Trench 4 (see Table 2). These suggest that, beginning around 7000 years ago, the occupations of La Yerba II represented by the stratigraphies of Trenches 1 and 3 took place over only 339 and 175 years, respectively: with maximum likely durations between their boundary limits of 545 and 445 years, respectively, see Table 2). Modelling Carré et al.'s (2012) previously published dates for Trench 4 suggest a time depth of occupation of 342 years between median boundary limits (or 1215 years maximum difference between boundary limits). These La Yerba II chronostratigraphies are each internally consistent and demonstrate that, in an exceptionally windy shoreline environment, human occupation promoted the accumulation of settlement detritus amidst constantly-aggrading, fine, wind-blown sands to build up some 5 m of tell-like mound stratigraphy in something less than five centuries (see Fig. 11). This rapid aggradation of stratigraphy suggests that La Yerba II's occupation followed an intense rhythm, consistent with our interpretation of it as a logistical basecamp from which marine hunter gatherers could engage in rounds of logistical mobility, while simultaneously reducing their residential mobility (cf. Jerardino, 2010, 2012; Standen et al., 2017).

Finally, the La Yerba II sequence also suggests some significant changes in economic behaviour through time. For whereas its underlying contexts reflect the aforementioned alternating episodes of occupation and abandonment, the uppermost contexts of Trenches 1 (SU 1001 and 1002, see Fig. 4A), and Trench 3 (SU 1053 and 1057, see Fig. 5A) are distinct: made up of thick accumulations of shells within a fabric of wind-blown unconsolidated sand (Fabric 1). SU 1001 and 1002, for instance, accounted for almost 60% by weight of all molluscs recovered in systematic sampling throughout all Trench 1's profile, and almost 80% of that overburden shell horizon was composed of a single species: *Mesodesma donacium* surf clams (77% by weight, see Fig. 8). These almost pure shell horizons SU 1002 and SU 1053 in Trenches 1 and 3 date to 6841–6638 cal BP and 6743–6503 cal BP, respectively (see Table 2, Fig. 7): marking a *terminus post quem* for the final phase of La Yerba II's occupation.

Only around three centuries later, Middle Preceramic occupation on the Río Ica estuary takes very different form at the site of La

Yerba III, around a kilometre upstream. Dating to between 6281 and 6095 cal BP, La Yerba III was a permanently, or nearly-permanently, settled village over some 4 ha and composed of many superimposed semi-subterranean dwellings and storage pits. Marine foods still underpinned the diet here, although apparently harvested with more sophisticated fabric technologies evidenced by a much greater proportion of smaller, schooling net-caught fish in the La Yerba III assemblage as compared with La Yerba II (Beresford-Jones et al., 2018). Moreover, these were supplemented by some food crops requiring cultivation, including domesticated lima beans ('pallar', *Phaseolus lunatus*), jack beans ('pallar del gentil' *Canavalia ensiformis*), guava (*Psidium guajava*); and animals in the form of guinea pigs (*Cavia porcellus*) and dogs (*Canis fammiliaris*). This unfolding trajectory on the Río Ica estuary towards increasing intensification and more permanent village settlement is reflected more widely along this Pacific coast (e.g. Beresford-Jones et al., 2021). Its antecedents may also be evident in La Yerba II's final contexts, whose composition of almost pure *Mesodesma* shell midden suggest more task-specific and/or season-specific activities than the more generalised logistical basecamp occupations revealed in its deeper, underlying stratigraphy.

4.4. Reconstruction of estuarine environment

Today La Yerba II lies almost a kilometre inland with its basal deposits almost 20m above mean sea level, on a relict marine terrace whose elevation corresponds to the well-expressed MiS 5e marine terrace feature mapped along the Peruvian coast Freisleben et al. (2021), Fig. 1), and in line with the elevation given by Garrett et al. (2020) for their marine limiting point for 7.2 k BP at Caleta Michilla, northern Chile. When it was occupied La Yerba II likely lay in immediate proximity to foreshore dunes behind the extant surf line, just like the Yamana shell middens described by Lothrop (1928: 179) in Tierra del Fuego: 'the seaward slopes of the middens are fronting the beach and stand so close to the waters that they are occasionally dashed with spray, and many are undercut by the waves for a foot or two at the base' (Fig. 3). La Yerba II's topographical position today is, then, the result of beach progradation following eustatic sea level stabilisation and a complex history of on-going tectonic uplift.

Fed by sediment from the river and a shallow offshire zone the immediate Río Ica estuary has experienced more beach development than any other location along this coast south of Paracas (Craig, 1968: 55). Reworked by on-shore winds this feeds dune formations, constrained laterally by predominant wind direction and local topography into a zone c. 5 km north and west and 9 km south and west of the current river mouth (Fig. 12A). This input of sediment was critical to the aggregation of the La Yerba II mound during its occupation. Subsequently it has helped preserve and protect it, along with other archaeological sites on the estuary.

The estuarine environment here can be hypothesised for the time of La Yerba II's occupation seven millennia ago using the AW3D DEM and a line of highest astronomical tide (HAT) inferred from ancient shoreline erosion features recorded with the RTK GPS and visible in the satellite and drone imagery; the lack of sorting in aeolian sediments throughout its contexts; and the evidence of Fuegian ethnographies. Similar to Garrett et al.'s (2020) reasoning for Caleta Michilla, this gives a regional limiting date and elevation for sea-level, rather than a more constrained index point. Indeed, the elevation of these features and local geomorphology suggest a possible palaeo-lagoon during MiS 5e, evolving into much more extensive estuarine marsh in the early-mid Holocene, than today (see Fig. 12 and cf. the raised coastal embayment noted at Otuma 120 km to the north, Craig, 1968: 100).

5. Conclusions

Dating to between 7011 and 6651 Cal BP the La Yerba II mound on the north bank of the Río Ica estuary is an early example of a Holocene shoreline archaeological record that, worldwide, rarely date to before 6000 BP because, until then, eustatic sea-levels had risen as the earth warmed through the early Holocene. Driven by this global eustatic sea level change the specifics of how shoreline morphology changed depended on local factors of bathymetry, tectonics, isostatic adjustment and sedimentary deposition. On coastline not directly impacted by ice coverage during the LGM such as the south coast of Peru, today's beaches and estuary only began to take on their recognisable form *after* six thousand years ago: a critical chronology because

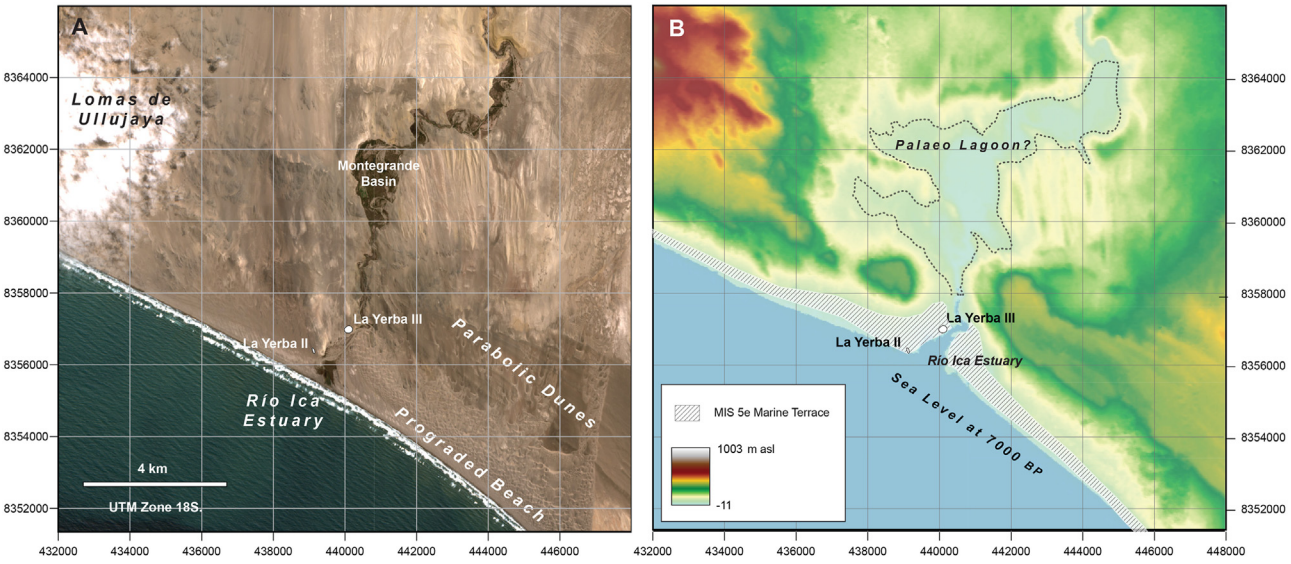

Fig. 12. (A) Sentintel-2 Copernicus (2021) image of the Rio Ica Estuary with major geomorphological features marked. (B) Hypothetical DEM model of sea-level and immediate La Yerba II environment during occupation at 7 k BP.

of the significance of resources from those particular habitats in La Yerba II's midden deposits: not least *Mesodesma* surf clams from the surf line along the beach and starchy rhizomes of *Cyperaceae esculentus* from estuarine wetlands.

La Yerba II's topographic position today, almost a kilometre behind today's shoreline on a well-defined MiS 5e marine terrace around 18 m AMSL evidence significant local processes of coastal morphological change at the Río Ica estuary. The geoarchaeological and ethnographic evidence presented here suggests that when La Yerba II was occupied, 7000 years ago it lay just above the extant HAT shoreline, alongside a significantly larger river estuary and palaeo-lagoon (see Fig. 12B). Its position today is the outcome of beach progradation and on-going tectonic uplift. Without more data on other local factors (such as sediment burden off the river mouth), it is not possible to determine precisely the on-going rate of tectonic uplift implied by La Yerba II's current position. However, along tectonically inactive coastlines such as South Africa, MiS 5e sea-level highstands are typically reported at between 6 and 8.5 m AMSL (e.g. Cawthra et al., 2018), implying a relative elevation of the MiS 5e terrace at the Río Ica estuary of between 11.7 and 9.5 at m AMSL and a rate of uplift here of around 1.7–1.3 m/ka (slightly higher, but of the same order of magnitude, as the estimates of Saillard et al. (2011) over the greater time depth of the Pleistocene).

The earliest occupation of La Yerba II is composed of elements of surfaces indurated with hydroxylapatite (e.g. SU 1083), along with ashy materials with abundant degraded and weathered bone and shell fragments (Fabrics 3 and 5): echoing characterisations of Archaic floor deposits in the Tlacuachero shell mound in Chiapas, Mexico (Neff et al., 2015). Thereafter the mound's stratigraphy accumulated rapidly. A tightly resolved chronostratigraphic framework provided by calibrating and Bayesian modelling of 25 radiocarbon dates as sequences of phases shows that at La Yerba II's highest point some 4.5 m of stratigraphy accumulated over only five centuries. The suite of geoarchaeological analyses presented here — including thin section micromorphology, FTIR and ICP-AES multi-element analyses — reveal that, in a very windy coastline environment, this rapid formation was the outcome the constant accumulation of wind-blown sediments promoted by an intense rhythm of repeated, small-scale occupations by logistically mobile marine hunter-gatherers.

Much of La Yerba II's shell-matrix (*sensu* Villagran, 2019: 345) stratigraphy is the palimpsest of sequences of occupation defined by prepared surfaces and indurated floors (Fabrics 4 and 5) and well-defined discontinuous ashy layers (Fabric 3). These are interpreted as the interiors of areesh-type wind shelters similar to those described in Fuegian contexts and their associated middens (Fabric 2), with some similarities also with the compacted living surfaces observed in Brazilian shell mounds (Villagran, 2019, 365: Microfacies A1). Interspersed with these were multiple phases of abandonment marked by deep horizons of wind blown unconsolidated sands (Fabric 1), almost barren of anthropologic indicators (see Fig. 11). We therefore interpret La Yerba II to have been a logistical basecamp, whose location at the confluence of salt and freshwater, and marine and terrestrial, habitats, enabled its occupants to reduce their residential mobility by exploiting diverse resources according to seasonal rounds of logistical mobility, evidenced in its midden assemblages from in-shore pelagic resources of beach and estuary, benthic habitats of rocky headlands and riverine and ephemeral *lomas* winter fog oases.

La Yerba II also sits on a trajectory towards increasing sedentism represented by the wider archaeological record of the Middle Preceramic along this Pacific coast (Moseley, 1975; Marquet et al., 2012; Standen et al., 2017). *Mesodesma* surf clams proliferate in vast beds in shallow waters off sandy beaches: habitats that formed and eroded with changing eustatic sea-level through the Early Holocene. These molluscs represented an ideal and almost inexhaustible source of protein for marine hunter-gatherers, easily collected without significant risk by all members of society, and easily and efficiently opened in bulk over small fires. *Mesodesma* are vulnerable to perturbations in sea temperature, although this far south this would occur during exceptionally powerful EP mode ENSO events.[2] Their ubiquity in the La Yerba II record, and indeed in earlier sites along this Pacific coast such Quebrada Jaguay (Sandweiss, personal communication), Quebrada de los Burros (Lavallée and Julien, 2012) and Abrigo I (Beresford-Jones et al., 2015), suggest that *Mesodesma* may have been the critical component of the rich array of marine resources that allowed marine hunter-gatherers along this coast to reduce mobility, enabled by colder seas persisting for millennia along this coast since the Early Holocene (Carré et al., 2014; Beresford-Jones et al., 2015). This process towards sedentism is perhaps also reflected in La Yerba II's final, thick shell-midden *sensu stricto* contexts which mark change from the generalised logistical basecamp occupations of its underlying stratigraphy towards a much more task-specific activities. For these middens are dominated by *Mesodesma,* whose sandy beach habitats began to prograde towards today's extent about the mouth of the Río Ica following the stabilisation of eustatic sea-levels after 6000 BP.

Indeed, only a few centuries after the deposition of La Yerba II's final surf-clam shell middens, occupation at the Río Ica estuary took new form in the permanent village of semi-subterranean houses at La Yerba III around a kilometre inland along the estuary: one of many settled villages that started to coalesce along this Pacific coast around 6000 BP which incorporated increasing amounts of cultivated food crops throughout the subsequent fifth millennium BP (Engel, 1991; Benfer, 2008; Dillehay, 2017; Gorbahn, 2020; Beresford-Jones et al., 2018, 2021). On the wide deltaic and lower river floodplains of the central and northern coasts of Peru, where flooding cycles brought rich alluvium and freshwater on which farming flourished, the conjunction of marine and terrestrial resources that had enabled increasing sedentism throughout the Middle Preceramic at sites such as La Yerba II were to find their ultimate expression in one of humanity's rare pristine civilisations (cf. Kennett and Kennett, 2006). The archaeological record of the La Yerba II shell midden on the Pacific coast of Peru thereby represents a classic example of the systematic broad-spectrum exploitation of marine and aquatic resources that defined a long Mesolithic prelude to agriculture in many places worldwide.

Author contributions

D.G. Beresford-Jones – paper design and writing, archaeological and geoarchaeological fieldwork, calibration and Bayesian modelling of radiocarbon dates, interpretations, project funding. D.E. Friesem – paper design and writing, geoarchaeological analyses, interpretations. F. Sturt – paper design and writing, archaeological survey and processing of survey data, DEM modelling, interpretations. A. Pullen – archaeological fieldwork, interpretations. G.E. Chauca – archaeological fieldwork, interpretations. J. Moat – drone survey data. M. Gorriti – malacological analysis. P. K. Maita – zooarchaeological analysis. D. Joly – charcoal analysis. O. Huaman – archaeological fieldwork. K.J. Lane – archaeological fieldwork and project funding. C.A.I. French – paper design and writing, geoarchaeological fieldwork, micromorphology analysis, interpretations, laboratory director, project funding.

[2] Intolerant of warmer seas, *Mesodesma donacium* disappeared from the south coast of Peru during the so-called mega-El Niño event of 1997–8 and have yet to return.

Declaration of competing interest

The authors declare that they have no known competing financial interests or personal relationships that could have appeared to influence the work reported in this paper.

Acknowledgments

We thank Daniel Sandweiss and two anonymous reviewers for their many useful suggestions on this paper; all the members of Cambridge University's One River Project; the *Ministerio de Cultura del Perú* for granting permission for archaeological fieldwork (under *Resolucion Directoral* No. 933-2012-DGPC-VMPCIC/MC, 19 December 2012) and the export of samples for dating; the director of the *Museo Regional de Ica* Susana Arce; Alberto Benavides G. and the people of Samaca; the Leverhulme Trust (grant number RPG-117); the late Don Alberto Benavides de la Quintana (grant number RG69428); and the NERC Radiocarbon facility (grant number NF/2013/2/2) for funding. We also thank Dr Tonko Rajkovača of the McBurney Laboratory for making thin sections; and the ALS Chemex Laboratory, Seville, Spain, for multi-element results.

Appendix A. Supplementary data

Supplementary data to this article can be found online at https://doi.org/10.1016/j.quascirev.2022.107509.

References

Adderley, W.P., Wilson, C.A., Simpson, I.A., Davidson, D.A., 2010. Anthropogenic features. In: Stoops, G., Marcelino, V., Mees, F. (Eds.), Interpretation of Micromorphological Features of Soils and Regoliths. Elsevier, Amsterdam, pp. 569–588.

Aldeias, V., Bicho, N., 2016. Embedded behavior: human activities and the construction of the Mesolithic Shellmound of Cabeço da Amoreira, Muge, Portugal. Geoarchaeology 31, 530–549.

Allen, M.J., Macphail, R.I., 1987. Micromorphology and magnetic susceptibility studies: their combined role in interpreting archaeological soils and sediments. In: Fedoroff, N., Bresson, L.M., Courty, M.A. (Eds.), Soil Micromorphology. Association Francaise pour l'Etude du Sol, Paris, pp. 669–676.

Arce, S., Pullen, A.G., Huaman, J.O., Chauca, G.E., Beresford-Jones, D.G., 2014. Proyecto de Investigación Arqueológica Samaca. Informe de los Trabajos Realizados en La Yerba II, Boca del Río Ica y Samaca H-8 durante la Temporada 2013. Presentado al Ministerio de Cultura Lima, Perú.

Bailey, G.N., Flemming, N.C., 2008. Archaeology of the continental shelf: marine resources, submerged landscapes and underwater archaeology. Quat. Sci. Rev. 27, 2153–2165.

Bailey, G., Hardy, K., 2021. Coastal prehistory and submerged landscapes: Molluscan resources, shell-middens and underwater investigations. Quat. Int. 584, 1–8.

Balbo, A.L., Madella, M., Vila, A., Estévez, J., 2010. Micromorphological perspectives on the stratigraphical excavation of shell middens: a first approximation from the ethnohistorical site Tunel VII, Tierra del Fuego (Argentina). J. Archaeol. Sci. 37, 1252–1259.

Bar-Yosef Mayer, D.E., Zohar, I., 2010. The role of aquatic resources in the Natufian culture. Eurasian Prehistory 7, 29–43.

Benfer, R.A., 2008. Early villages. In: Persall, D.M. (Ed.), Encyclopedia of Archaeology, vol. 1. Academic Press, New York, pp. 368–380.

Beresford-Jones, D.G., Pullen, A.G., Whaley, O.Q., Moat, J., Chauca, G., Cadwallader, L., Arce, S., Orellana, A., Alarcón, C., Gorriti, M., Maita, P., Sturt, F., Dupeyron, A., Huaman, O., Lane, K.J., French, C., 2015. Re-evaluating the resource potential of lomas fog oasis environments for preceramic hunter-gatherers under past ENSO modes on the south coast of Peru. Quat. Sci. Rev. 129, 196–215.

Beresford-Jones, D.G., Pullen, A.G., Chauca, G., Cadwallader, L., García, M., Salvatierra, I., Whaley, O.Q., Vásquez, V., Arce, S., Lane, K.J., French, K.J., 2018. Refining the maritime foundations of Andean civilization: how plant fiber technology drove social complexity during the Preceramic period. J. Archaeol. Method Theor 25, 393–425.

Beresford-Jones, D.G., Pomeroy, E., Alday, C., Benfer, R.A., Quilter, J., O'Connell, T., Lightfoot, E., 2021. Diet and lifestyle in the first villages of the Middle Preceramic: insights from stable Isotope and osteological analyses of human remains from Paloma, Chilca I, La Yerba III and Morro I. Lat. Am. Antiq. 32 (2), 741–759. https://doi.org/10.1017/laq.2021.24.

Bicho, N., Haws, J.A., Davis, L.G. (Eds.), 2011. Trekking the Shore, Changing Coastlines and the Antiquity of Coastal Settlement. Springer, New York.

Binford, L.R., 1968. Post-Pleistocene adaptations. In: Binford, S.R., Binford, L.R. (Eds.), New Perspectives in Archaeology. Aldine Publishing, Chicago, pp. 313–342.

Binford, L.R., 1980. "Willow smoke and dogs" tails: hunter-gatherer settlement systems and archaeological site formation. Am. Antiq. 45, 4–20.

Blanco-Chao, R., Pedoja, K., Witt, C., Martinod, J., Husson, L., Regard, V., Audin, L., Nexer, M., Delcaillau, B., Saillard, M., Melnick, D., 2014. The rock coast of South and Central America. Geological Society, London, Memoirs 40 (1), 155–191.

Borreggine, M., Powell, E., Pico, T., Mitrovica, J.X., Meadow, R., Tryon, C., 2022. Not a bathtub: a consideration of sea-level physics for archaeological models of human migration. J. Archaeol. Sci. 137, 105507.

Bradley, R., 1984. The Social Foundations of British Prehistory. Longman.

Bronk Ramsey, C., 2009. Bayesian analysis of radiocarbon dates. Radiocarbon 51, 337–360.

Bronk Ramsey, C., Higham, T.F.G., Owen, D.C., Pike, A.W.G., Hedges, R.E.M., 2002. Radiocarbon dates from the Oxford AMS system, archaeometry datelist 31. Archaeometry 44 (Suppl. 1), 1–149.

Bronk Ramsey, C., Higham, T.F.G., Leach, P., 2004. Towards high-precision AMS: progress and limitations. Radiocarbon 46, 17–24.

Carmichael, P.H., Cordy-Collins, A., 2020. Prehistory of the Ica-Nazca Littoral, Peru. Andean Past Special Publications, 7. https://digitalcommons.library.umaine.edu/andean_past_special/7.

Carré, M., Sachs, J.P., Purca, S., Schauer, A.J., Braconnot, P., Falcon, R.A., Julien, M., Lavallee, D., 2014. Holocene history of ENSO variance and asymmetry in the eastern tropical Pacific. Science 345, 1045–1048.

Carré, M., Azzoug, A., Bentaleb, I., Chase, B.M., Fontugne, M., Jackson, D., Ledru, M.-P., Maldonado, A., Sach, J.P., Schauer, A.J., 2012. Mid-Holocene mean climate in the south eastern Pacific and its influence on South America. Quat. Int. 253, 55–66.

Casavilca Curaca, A., 1958. Una exploración paleontológica y arqueológica en que fueron descubiertos los primeros fósiles vertebrados del Perú y restos del período pre-cerámico de Ica. Actas y Trabajos del II Congreso Nacional de Historia del Perú (Época Prehispánica) 1, 298–303.

Castro, V., Aldunate, C., Varela, V., Olguín, L., Andrade, P., García-Albarido, F., Rubio, F., Castro, P., Maldonado, A., Ruz, J., 2016. Ocupaciones arcaicas y probables evidencias de navegación temprana en la costa arreica de Antofagasta, Chile. Chungará 48, 503–530.

Chauca, G., Glascock, M.D., Rodríguez, J., Arce, S., Beresford-Jones, D.G., 2019. El vidrio volcánico del litoral de Ica durante el Precerámico Medio (8000–5000 AP). In: Actas del V Congreso Nacional de Arqueología, vol. I. Ministerio de Cultura, Lima, Perú, pp. 177–185.

Cawthra, H.C., Jacobs, Z., Compton, J.S., Fisher, E.C., Karkanas, P., Marean, C.W., 2018. Depositional and sea-level history from MIS 6 (Termination II) to MIS 3 on the southern continental shelf of South Africa. Quat. Sci. Rev. 181, 156–172.

Cook, A.G., 1994. Invesitigaciones de Reconocimiento Arqueologico en la Parte Baja del Valle de Ica. Informe Final (1988-1990). Instituto Nacional de Cultura, Lima.

Cooke, R.U., Warren, A., Goudie, A.S., 1993. Desert Geomorphology. University College London Press, London UK.

Courty, M.-A., 2001. Microfacies analysis assisting archaeological stratigraphy. In: Goldberg, P., Holliday, V.T., Reid Ferring, C. (Eds.), Earth Sciences and Archaeology. Kluwer, New York, pp. 205–239.

Craig, A.K., 1968. Marine desert ecology of southern Peru (Vol. 1, No. 2), 2nd. Office of Naval Research, Geography Branch. No. 2.

Culleton, B., Voorhies, B., Kennett, D.J., 2015. Stratigraphy and chronology of the Archaic Period deposits at Tlacuachero. In: Voorhies, B. (Ed.), An Archaic Mexican Shellmound and its Entombed Floors. University of California, Los Angeles, pp. 19–29. Monograph 80.

Day, J.W., Yanez-Arancibia, A., Kemp, M., Crump, B.C., 2012. Estuarine Ecology. J. Wiley & Sons, New York.

De Vynck, J.C., Anderson, R., Atwater, C., Cowling, R.M., Fisher, E.C., Marean, C.W., Walker, R.S., Hill, K., 2016. Return rates from intertidal foraging from Blombos Cave to Pinnacle Point: understanding early human economies. J. Hum. Evol. 92, 101–115.

Dillehay, T.D., Bonavia, D., Goodbred, S., Pino, M., Vasquez, V., Rosales Tham, T., Conklin, W., Splitstoser, J., Piperno, D., Iriarte, J., Grobman, A., Levi-Lazzaris, G., Moreira, D., Lopéz, M., Tung, T., Titelbaum, A., Verano, J., Adovasio, J., Scott-Cummings, L., Bearéz, P., Dufour, E., Tombret, O., Ramirez, M., Beavins, R., DeSantis, L., Rey, I., Mink, P., Maggard, G., Franco, T., 2012. Chronology, mound-building, and environment at Huaca Prieta, coastal Peru, from 13,700 to 4,000 years ago. Antiquity 86, 48–70.

Dillehay, T.D. (Ed.), 2017. Where the Land Meets the Sea: Fourteen Millennia of Human History at Huaca Prieta, Peru. University of Texas Press, Austin.

Duarte, C., Iriarte, E., Diniz, M., Arias, P., 2019. The microstratigraphic record of human activities and formation processes at the Mesolithic shell midden of Poças de São Bento (Sado Valley, Portugal). Archaeolog. Anthropol. Sci. 11, 483–509.

Engel, F.A., 1981. Prehistoric Andean Ecology. Man, Settlement and Environment in the Andes. The Deep South. Humanities Press, Hunter College, New York.

Engel, F.A., 1991. Un Desierto en Tiempos Prehispánicos. La Universidad Nacional Agraria Del Perú, Lima, Perú.

Esteban, I., Bamford, M.K., House, A., Miller, C.S., Neumann, F.H., Schefuß, E., Pargeter, J., Cawthra, H.C., Fisher, E.C., 2020. Coastal palaeoenvironments and hunter-gatherer plant-use at Waterfall bluff rockshelter in Mpondoland (South Africa) from MIS3 to the early Holocene. Quat. Sci. Rev. https://doi.org/10.1016/j.quascirev.2020.106664.

Estévez, J., Vila, A., 2006. Variability in the lithic and faunal record through 10 reoccupations of a XIX century Yamana Hut. J. Anthropol. Archaeol. 25, 408–423.

FAO, 2014. Fish, Crustaceans, Molluscs, etc.: Capture Production by Principal Species

in 2012 FAO Fisheries Statistics. ftp://ftp.fao.org/FI/STAT/summary/a1e.pdf. (Accessed 12 October 2014).
Fish, S.K., De Blasis, P., Gaspar, M.D., Fish, P.R., 2000. Eventos incrementais na construção de sambaquis, litoral sul do estado de Santa Catarina, vol. 10. Revista do Museu de Arqueologia e Etnologia, pp. 69–87.
Fisher, E.C., Cawthra, H.C., Esteban, I., Jerardino, A., Neumann, F.H., Oertlef, A., Pargeter, J., Saktura, R.B., Szabó, K., Winkler, S., Zohar, I., 2020. Coastal occupation and foraging during the last glacial maximum and early Holocene at Waterfall Bluff, eastern Pondoland, South Africa. Quat. Res. 1–41. https://doi.org/10.1017/qua.2020.26.
Flannery, K.V., 1969. In: Ucko, P., Dimbleby, G.W. (Eds.), The Domestication and Exploitation of Plants and Animals. Duckworth, pp. 73–100.
Freisleben, R., Jara-Muñoz, J., Melnick, D., Martínez, J.M., Strecker, M.R., 2021. Marine terraces of the last interglacial period along the Pacific coast of South America (1° N–40° S). Earth Syst. Sci. Data 13, 2487–2513.
Friesem, D.E., Tsartsidou, G., Karkanas, P., Shahack-Gross, R., 2014. Where are the roofs? A geo-ethnoarchaeological study of mud brick structures and their collapse processes, focusing on the identification of roofs. Archaeolog. Anthropol. Sci. 6, 73–92.
Friesem, D.E., Lavi, N., Madella, M., Ajithprasad, P., French, C., 2016. Site formation processes and hunter-gatherers use of space in a tropical environment: a geo-ethnoarchaeological approach from South India. PLoS One 11, e0164185. https://doi.org/10.1371/journal.pone.0164185.
Friesem, D.E., Lavi, N., Madella, M., Boaretto, E., Ajithparsad, P., French, C., 2017. The formation of fire residues associated with hunter-gatherers in humid tropical environments: a geo-ethnoarchaeological perspective. Quat. Sci. Rev. 171, 85–99.
Garrett, E., Melnick, D., Dura, T., Cisternas, M., Ely, L.L., Wesson, R.L., Jara-Muñoz, J., Whitehouse, P.L., 2020. Holocene relative sea-level change along the tectonically active Chilean coast. Quat. Sci. Rev. 236, 106281.
Gaspar, M.D., DeBlasis, P., Fish, S.K., Fish, P.R., 2008. Sambaqui (shell mound) societies of coastal Brazil. In: Silverman, H., Isbell, W.H. (Eds.), Handbook of South American Archaeology. Springer, New York, pp. 319–337.
Ge, T., Courty, M.A., Matthews, W., Wattez, J., 1993. Sedimentary formation processes of occupation surfaces. In: Goldberg, P., Nash, D.T., Petraglia, M.D. (Eds.), *Formation Processes in Archaeological Context*. Monographs in World Archaeology 17, 149–164.
Gorbahn, H., 2020. Pernil Alto: An Agricultural Village of the Middle Archaic Period in Southern Peru. Forschungen zur Archäologie Außereuropäischer Kulturen Band, vol. 17. Harrassowitz, Wiesbaden.
Goy, J., Macharé, J., Ortlieb, L., Zazo, C., 1992. Quaternary shorelines in southern Peru: A record of global sea-level fluctuations and tectonic uplift in Chala Bay. Quaternary International 15, 99–112.
Harff, J., Bailey, G.N., Lüth, F., 2016. Late Quaternary beach deposits and archaeological relicts on Cyprus coasts and the possible implications of sea level changes and tectonics on the early populations. In: Harff, J., Bailey, G.N., Lüth, F. (Eds.), Geology and Archaeology: Submerged Landscapes of the Continental Shelf. Geological Society of London, London, UK, pp. 1–8. Special Publications (411).
Hogg, A.G., Heaton, T., Hua, Q., Palmer, J., Turney, C.S.M., Southon, J., Bayliss, A., Blackwell, P., Boswijk, G., Bronk Ramsey, C., Petchey, F., Reimer, P.J., Reimer, R.W., Wacker, L., 2020. SHCal20 Southern Hemisphere calibration, 0–55,000 years cal BP. Radiocarbon 62, 759–778.
Hsu, J.T., 1992. Quaternary uplift of the Peruvian coast related to the subduction of the Nazca ridge: 13.5 to 15.6 degrees south latitude. Quat. Int. 15/16, 87–97.
Isla, F.I., Flory, J.Q., Martínez, C., Fernandez, A., Jaque, E., 2012. The evolution of the Bío Bío delta and the coastal plains of the Arauco Gulf, Bío Bío Region: the Holocene sea-level curve of Chile. J. Coast. Resour. 28, 102e111.
Jerardino, A., 2010. Large shell middens in Lamberts Bay, South Africa: a case of hunter-gatherer resource intensification. J. Archaeol. Sci. 37, 2291–2302.
Jerardino, A., 2012. Large shell middens and hunter-gatherer resources intensification along the west coast of South Africa: the Elands Bay case study. J. I. Coast Archaeol. 7, 76–101.
Jerardino, A., Navarro, R., 2018. Large-scale hunter-gatherer exploitation of marine resources in South Africa, Part II: Grootrif and Malkoppan megamiddens, Lamberts Bay area. S. Afr. Archaeol. Bull. 73, 108–125.
Karkanas, P., Goldberg, P., 2010. Phosphatic features. In: Stoops, G., Marcelino, V., Mees, F. (Eds.), Interpretation of Micromorphological Features of Soils and Regoliths. Elsevier, Amsterdam, pp. 521–542.
Karkanas, P., Goldberg, P., 2018. Reconstructing Archaeological Sites: Understanding the Geoarchaeological Matrix. John Wiley & Sons, London.
Karkanas, P., Brown, K.S., Fisher, E.C., Jacobs, Z., Marean, C.W., 2015. Interpreting human behavior from depositional rates and combustion features through the study of sedimentary microfacies at site Pinnacle Point 5-6, South Africa. J. Hum. Evol. 85, 1–21.
Kennett, D.J., Culleton, B.J., 2012. A Bayesian chronological framework for determining site seasonality and contemporaneity. Seasonality and human mobility along the Georgia Bight. Am. Museum Nat. History Anthropol. Paper. 97, 37–50.
Kennett, D.J., Kennett, J.P., 2006. Early state formation in southern Mesopotamia: Sea levels, shorelines, and climate change. J. I. Coast Archaeol. 67–99.
Klokler, D., 2014. A ritually constructed shell mound. In: Roksandic, M., Mendoza de Souza, S., Eggers, S., Buschnell, M., Klokler, D. (Eds.), The Cultural Dynamics of Shell-Matrix Sites. University of New Mexico Press, Albuquerque, pp. 151–162.
Kroeber, A.L., Strong, W.D., Uhle, M., 1924. Uhle Pottery Collections from Ica, vol. 21. University of California Publications in American Archaeology, pp. 95–133.
Lanning, E., 1967. Peru before the Incas. Prentice Hall, Englewood Cliffs, N.J.
Lavallée, D., Julien, M. (Eds.), 2012. Prehistoria de la costa extremo-sur del Perú: los pescadores arcaicos de la Quebrada de los Burros (1000-7000 a.P.). Instituto Francés de Estudios Andinos, Lima, Perú.
Linstädter, J., Kehl, M., 2012. The Holocene archaeological sequence and sedimentological processes at Ifri Oudadane, NE Morocco. J. Archaeol. Sci. 39, 3306–3323.
Lewis, J.P., Ryves, D.B., Rasmussen, P., Olsen, J., van der Sluis, L.G., Reimer, P.J., Knudsen, K.-L., McGowan, S., Anderson, N.J., Juggins, S., 2020. Marine resource abundance drove pre-agricultural population increase in Stone Age Scandinavia. Nat. Commun. 11. https://doi.org/10.1038/s41467-020-15621-1.
Lothrop, S.K., 1928. The Indians of Tierra Del Fuego, Contributions from the Museum of the American Indian Heye Foundation. Lancaster Press, INC, Lancaster, PA.
McLaren, S.J., 1995. The role of sea spray in vadose diagenesis in Late Quaternary coastal deposits. J. Coast Res. 11, 1075–1088.
McLusky, D.S., Elliott, M., 2004. The Estuarine Ecosystem. Oxford University Press, Oxford.
Marean, C.W., 2014. The origins and significance of coastal resource use in Africa and Western Eurasia. J. Hum. Evol. 77, 17–40.
Marquardt, W., 2010. Shell mounds in the southeast: middens, monuments, temple mounds, rings, or works? Am. Antiq. 75, 551–570.
Marquet, P.A., Santoro, C.M., Latorre, C., Standen, V.G., Abades, S.R., Rivadeneira, M.M., Arriaza, B., Hochberg, M.E., 2012. Emergence of social complexity among coastal hunter-gatherers in the Atacama Desert of northern Chile. Proc. Natl. Acad. Sci. Unit. States Am. 109, 14754–14760.
Mauricio, A.C., Grieseler, R., Heller, A.R., Kelley, A.R., Rumiche, F., Sandweiss, D.H., Viveen, W., 2021. The earliest adobe monumental architecture in the Americas. Proc. Natl. Acad. Sci. Unit. States Am. 118, e2102941118.
MOLAS, 1994. Archaeological Site Manual, third ed. Museum of London Archaeological Service. Museum of London, UK.
Morello, F., Torres, J., Martinez, I., Rodriguez, K., Arroyo-Kalin, M., French, C., Sierpe, V., San Roman, M., 2012. Punta Santa Ana archaeology: reconstruction of marine hunter-gatherer occupation sequences from the Magellan Strait, southernmost Patagonia, Chile. Magallania 40, 129–149.
Moseley, M.E., 1975. The Maritime Foundations of Andean Civilization. Cummings Publishing Company, Menlo Park, California.
Neves, W.A., Wesolowski, V., 2002. Economy, nutrition and disease in prehistoric coastal Brazil: a case study from the state of Santa Catarina. In: Steckel, R.H., Rose, J.C. (Eds.), The Backbone of History. Cambridge University Press, Cambridge, pp. 376–402.
Neff, H., Burger, P., Kott, I., 2015. Geochemistry of the Tlacuachero floors. In: Voorhies, B. (Ed.), An Archaic Mexican Shellmound and its Entombed Floors. University of California, Los Angeles, pp. 71–84. Monograph 80.
Ozán, I.L., French, C.A.I., Morello Repetto, F., Vásquez, C.A., Luppo, T., 2015. Coastal Occupations in Tierra del Fuego, Southernmost South America: a Late Holocene Hunter-Gatherer Context at Marazzi 2. Geoarchaeology 30, 465–482.
Parkington, J.E., Fisher, J.W., Tonner, T.W.W., 2009. "The fires are constant, the shelters are whims": a feature map of Later Stone Age camp sites at the Dunefield Midden site, Western Cape Province, South Africa. S. Afr. Archaeol. Bull. 64, 104–121.
Parsons, M.H., 1970. Preceramic subsistence on the Peruvian coast. Am. Antiq. 35, 292–304.
Power, X., Sitzia, L., Yrarrázaval, Salazar, D., Andrade, P., Hernández, V., Aliste, C., Muth, X., 2021. Ritual stone-built architecture and shell midden foundation: a semi-subterranean structure in hyperarid Atacama Desert coast, Northern Chile. Geoarchaeology. https://doi.org/10.1002/gea.21857.
Regard, V., Martinod, J., Saillard, M., Carretier, S., Leanni, L., Hérail, G., Audin, L., Pedoja, K., 2021. Late Miocene-Quaternary forearc uplift in southern Peru: new insights from 10Be dates and rocky coastal sequences. J. S. Am. Earth Sci. 109, 103261.
Saillard, M., Hall, S.R., Audin, L., Farber, D.L., Regard, V., Hérail, G., 2011. Andean coastal uplift and active tectonics in southern Peru: 10Be surface exposure dating of differentially uplifted marine terrace sequences (San Juan de Marcona, ~15.40S). Geomorphology 128, 178–190.
Salazar, D., Figueroa, V., Andrade, P., Salinas, H., Olguín, L., Power, X., Robelledo, S., Parra, S., Orellana, H., Urrea, J., 2015. Cronología y organización económica de las poblaciones arcaicas de la costa de Taltal. Estud. Atacameños 50, 7–46.
Sandweiss, D.H., 2003. Terminal Pleistocene through Mid-Holocene archaeological sites as paleoclimatic archives for the Peruvian coast. Palaeogeogr. Palaeoclimatol. Palaeoecol. 194, 23–40.
Sandweiss, D.H., 2009. Early fishing and inland monuments: challenging the maritime foundations of Andean civilization? In: Marcus, J., Williams, P.R. (Eds.), Andean Civilization. A Tribute to Michael Moseley. Cotsen Institute of Archaeology, University of California, Los Angeles, pp. 39–54. Monograph 63.
Sandweiss, D.H., McInnis, H., Burger, R.L., Cano, A., Ojeda, B., Paredes, R., Sandweiss, M.C., Glascock, M.D., 1998. Quebrada Jaguay: early south American maritime adaptations. Science 281, 1830–1832.
Santoro, C.M., Gayo, E.M., Carter, C., Standen, V.G., Castro, V., Valenzuela, D., De Pol-Holz, R., Marquet, P.A., Latorre, C., 2017. Loco or No Loco? Holocene climatic fluctuations, human demography, and community based management of coastal resources in northern Chile. Front. Earth Sci. 5, 77.
Standen, V., Santoro, C., Arriaza, B.T., Colleman, D., 2017. Hunting, gathering, fishing on the coast of the Atacama Desert: Chinchorro population mobility patterns inferred from strontium isotopes. Geoarchaeology 33, 162–176.
Stein, J.K. (Ed.), 1992. Deciphering a Shell Midden. Academic Press, San Diego,

California.
Stein, J.K., Green, D., Sherwood, S., 2011. Sediment analysis. In: Taylor, A., J K, S. (Eds.), Is it a House? Archaeological Excavations at English Camp, San Juan Island, Washington. University of Washington Press, Seattle, pp. 45–63.
Stiner, M.C., 2001. Thirty years on the "Broad Spectrum Revolution" and paleolithic demography. Proc. Natl. Acad. Sci. Unit. States Am. 98, 6993–6996.
Stiner, M.C., Bicho, N.F., Lindly, J., Ferring, R., 2003. Mesolithic to Neolithic transitions: new results from shell middens in the western Algarve, Portugual. Antiquity 77, 75–86.
Thompson, V.D., Marquardt, W.H., Cherkinsky, A., Roberts Thompson, A.D., Walker, K.J., Newsom, L.A., Savarese, M., 2016. From shell midden to midden-mound: the geoarchaeology of mound key, an Anthropogenic Island in Southwest Florida, USA. PLoS One 11 (4), e0154611.
Villagran, X.S., Schaefer, C.E.G.R., Ligouis, B., 2013. Living in the cold: Geoarchaeology of sealing sites from Byers peninsula (Livingston Island, Antarctica). Quat. Int. 315, 184–199.
Villagran, X.S., 2014. A redefinition of waste: deconstructing shell and fish mound formation among coastal groups of southern Brazil. J. Anthropol. Archaeol. 36, 211–227.
Villagran, X.S., 2019. The shell midden conundrum: comparative micromorphology of shell-matrix sites from South America. J. Archaeol. Method Theor 26, 344–395.
Villagran, X.S., Balbo, A.L., Madella, M., Vila, A., Estevez, J., 2011. Stratigraphic and spatial variability in shell middens: microfacies identification at the ethnohistoric site Tunel VII (Tierra del Fuego, Argentina). Archaeolog. Anthropol. Sci. 3, 357–378.
Voorhies, B., 2015. Site formation process and function at mega-shellmounds: refuse heaps or platform mounds? In: Voorhies, B. (Ed.), An Archaic Mexican Shellmound and its Entombed Floors. University of California, Los Angeles, pp. 193–207. Monograph 80.
Waselkov, G.A., 1987. Shellfish gathering and shell midden archaeology. Adv. Archaeol. Method Theor. 10, 93–210.
Weiner, S., 2010. Microarchaeology: Beyond the Visible Archaeological Record. Cambridge University Press, Cambridge.
Zangrando, A.F.J., Tivoli, A.M., Alunni, D.V., Pérez, S.A., Martinoli, M.P., Vargas, G.P., 2021. Exploring shell midden formation through tapho-chronometric tools: a case study from Beagle Channel, Argentina. Quat. Int. 584, 33–43.
Zeder, M.A., 2012. The Broad Spectrum Revolution at 40: resource diversity, intensification, and an alternative to optimal foraging explanations. J. Anthropol. Archaeol. 31, 241–264.